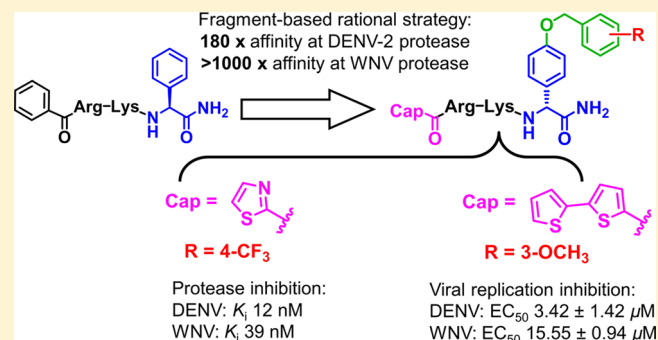


Discovery of Nanomolar Dengue and West Nile Virus Protease Inhibitors Containing a 4-Benzyloxyphenylglycine Residue

Mira A. M. Behnam,[†] Dominik Graf,[†] Ralf Bartenschlager,^{‡,||} Darius P. Zlotos,[§] and Christian D. Klein^{*,†}[†]Medicinal Chemistry, Institute of Pharmacy and Molecular Biotechnology IPMB, Heidelberg University, Im Neuenheimer Feld 364, 69120 Heidelberg, Germany[‡]Department of Infectious Diseases, Molecular Virology, Heidelberg University, Im Neuenheimer Feld 345, 69120 Heidelberg, Germany^{||}German Center for Infection Research, Heidelberg University, Im Neuenheimer Feld 345, 69120 Heidelberg, Germany[§]Department of Pharmaceutical Chemistry, The German University in Cairo, New Cairo City, 11835 Cairo, Egypt

Supporting Information

ABSTRACT: The dengue virus (DENV) and West Nile Virus (WNV) NS2B-NS3 proteases are attractive targets for the development of dual-acting therapeutics against these arboviral pathogens. We present the synthesis and extensive biological evaluation of inhibitors that contain benzyl ethers of 4-hydroxyphenylglycine as non-natural peptidic building blocks synthesized via a copper-complex intermediate. A three-step optimization strategy, beginning with fragment growth of the C-terminal 4-hydroxyphenylglycine to the benzyloxy ether, followed by C- and N-terminal optimization, and finally fragment merging generated compounds with in vitro affinities in the low nanomolar range. The most promising derivative reached K_i values of 12 nM at the DENV-2 and 39 nM at the WNV proteases. Several of the newly discovered protease inhibitors yielded a significant reduction of dengue and West Nile virus titers in cell-based assays of virus replication, with an EC_{50} value of 3.4 μ M at DENV-2 and 15.5 μ M at WNV for the most active analogue.

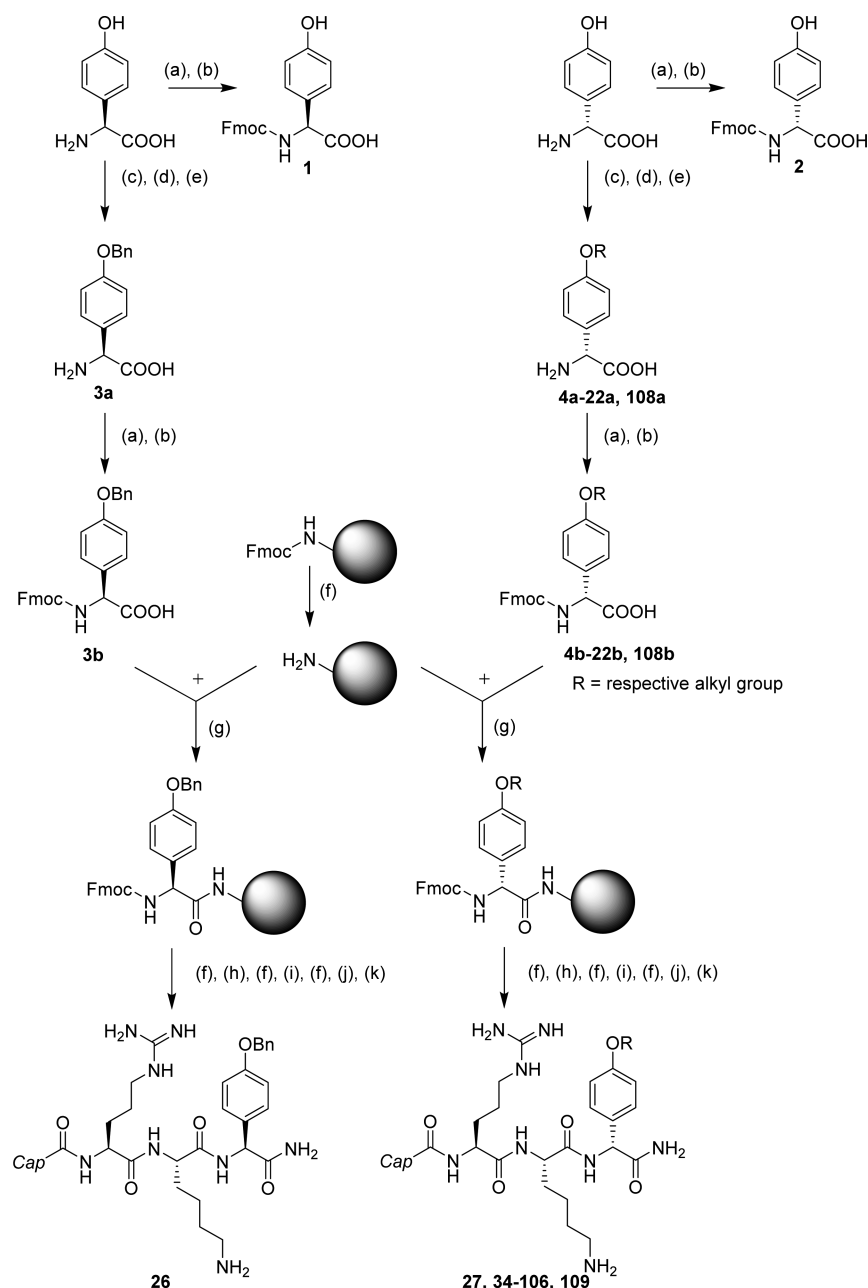


INTRODUCTION

Dengue virus (DENV) is the arthropod-borne virus (arbovirus) with the utmost impact on public health. Infection with DENV can cause a spectrum of symptoms ranging from the most common dengue fever, an acute self-limiting febrile illness, to the more severe and potentially fatal dengue hemorrhagic fever (DHF) and dengue shock syndrome (DSS). With an estimate of 50–100 million infections annually¹ and a recent analysis suggesting a higher infection burden of 390 million cases in 2010,^{2,3} dengue is prioritized by the World Health Organization (WHO) among 17 neglected tropical diseases. A related, medically relevant arboviral pathogen is the West Nile virus (WNV). Infection with WNV is sometimes asymptomatic but can develop into flu-like illness and fatal WNV neuroinvasive disease.⁴ Global warming, climate changes, increased global travel, urbanization, and insufficient vector control cause a continuous habitat expansion of the disease-transmitting mosquito vectors (*Aedes* and *Culex* spp.). This results in the rapid spread of infections beyond their original geographical boundaries.^{5,6} The development of antiviral chemotherapeutics or vaccines against dengue and WNV remains a critical, unmet medical need.

Both DENV and WNV belong to the *Flaviviridae* family, together with the hepatitis C virus (HCV) and several other pathogenic viruses. There are four related, yet antigenically distinct serotypes of dengue (DENV 1–4), in addition to an emerging fifth serotype.⁷ The flavivirus genome consists of a positive single-stranded RNA, which is translated into a precursor polyprotein. The latter is then cleaved co- and post-translationally, resulting in a small number of structural and nonstructural (NS) proteins. The NS3 protein contains a serine protease domain, whose activity depends on the formation of a noncovalent complex with the NS2B protein as cofactor.^{8–10} The NS2B-NS3 complex is responsible for the proteolytic processing of the viral polyprotein. It is hence crucial for virus replication and represents a promising target for the development of antiviral drugs. Protease inhibition was shown to be a successful strategy in the treatment of HIV and HCV infections,^{11–13} with most approved candidates being substrate-mimetics. While DENV and WNV proteases have similarities in their binding pockets that can potentially be used to develop dual inhibitors, they also share the challenges of

Received: September 16, 2015

Scheme 1^a

^aSpheres represent Rink amide resin particles. (a) H₂O/ACN, DIPEA, Fmoc-OSu; (b) HCl; (c) NaOH, CuSO₄·5H₂O; (d) NaOH, MeOH, respective alkylating agent, rt, 18 h; (e) HCl or 8-hydroxyquinoline; (f) piperidine, DMF; (g) HATU, DIPEA, DMF; (h) Fmoc-Lys(Boc)-OH, HATU, DIPEA, DMF; (i) Fmoc-Arg(Pbf)-OH, HATU, DIPEA, DMF; (j) Cap-COOH, HATU, DIPEA, DMF; (k) TFA, H₂O, TIPS (95:4:1 v/v, 2 h, rt).

possessing a solvent-exposed, topologically shallow active site and a selectivity for substrates containing basic amino acids (arginine and lysine) at P₁ and P₂.^{14,15} These highly polar groups account for the insufficient membrane permeability and poor pharmacokinetic profile of substrate-based inhibitors, despite their promising in vitro binding affinities. Both proteases are inhibited by the polypeptide aprotinin,^{16,17} in addition to various classes of nonpeptidic and peptidic inhibitors.^{17–23}

Potent peptidic inhibitors were obtained for the DENV-2^{24,25} and WNV²⁶ proteases by attaching a C-terminal, serine-reactive electrophilic functionality to an *N*-benzoyl capped tetrapeptide

sequence (Nle-Lys-Arg-Arg). This sequence contains the favored amino acids for the S₁–S₄ subsites of the protease binding cavity.^{16,27,28} For DENV-2, we found the benzoyl-capped retro-tripeptide lacking one arginine (Bz-Arg-Lys-Nle-NH₂) to be superior in terms of inhibitory activity, and this was chosen as the standard sequence for our subsequent work.²⁹ Our efforts to enhance activity and membrane permeability span between optimizing the *N*-terminal capping group and, more recently, the *C*-terminal residue. At the *N*-terminus, thiazolidinedione-capped peptide hybrids bearing hydrophobic substituents showed promising in vitro affinities at DENV-2 protease but displayed much lower inhibition at WNV

Table 1. Inhibitory Activity of Various *N*-Benzoyl-Capped Tripeptide Sequences against DENV and WNV Proteases

| no. | sequence | DENV | | WNV | |
|-----------------|--|----------------|------------------------------------|----------------|------------------------------------|
| | | % ^a | IC ₅₀ (μM) ^b | % ^c | IC ₅₀ (μM) ^d |
| I ³¹ | Bz-Arg-Lys-L-Phg-NH ₂ | 95.0 | 3.323 | 39.3 | 58.10 |
| 23 | Bz-Arg-Lys-D-Phg-NH ₂ | 99.3 | 3.790 | 99.0 | 3.780 |
| 24 | Bz-Arg-Lys-(4-OH)-L-Phg-NH ₂ | 96.6 | 9.695 | 79.2 | n.d. |
| 25 | Bz-Arg-Lys-(4-OH)-D-Phg-NH ₂ | 98.0 | 2.032 | 75.1 | n.d. |
| 26 | Bz-Arg-Lys-(4-benzyloxy)-L-Phg-NH ₂ | 99.9 | 0.935 | 88.0 | n.d. |
| 27 | Bz-Arg-Lys-(4-benzyloxy)-D-Phg-NH ₂ | 100.1 | 0.367 | 101.2 | 0.728 |
| 28 | Bz-Lys-(4-benzyloxy)-D-Phg-NH ₂ | 16.4 | n.d. | 11.4 | n.d. |
| 29 | Bz-Arg-(4-benzyloxy)-D-Phg-NH ₂ | 31.0 | n.d. | 27.5 | n.d. |
| 30 | Bz-Lys-Arg-(4-benzyloxy)-D-Phg-NH ₂ | 77.0 | n.d. | 91.7 | n.d. |
| 31 | Bz-D-Lys-D-Arg-(4-benzyloxy)-D-Phg-NH ₂ | 26.8 | n.d. | 19.9 | n.d. |
| 32 | Bz-D-Arg-D-Lys-(4-benzyloxy)-L-Phg-NH ₂ | 29.4 | n.d. | 71.3 | n.d. |
| 33 | Bz-D-Lys-D-Arg-(4-benzyloxy)-L-Phg-NH ₂ | 23.5 | n.d. | 64.0 | n.d. |

^aPercent inhibition of DEN NS2B-NS3 protease serotype 2 (inhibitor 50 μM, substrate 50 μM). ^bIC₅₀ values against DEN NS2B-NS3 protease serotype 2 at 50 μM substrate concentration. ^cPercent inhibition of WNV NS2B-NS3 protease (inhibitor 50 μM, substrate 50 μM). ^dIC₅₀ values against WNV NS2B-NS3 protease at 50 μM substrate concentration. n.d. = IC₅₀ was not determined for compounds with less than 95% inhibition. All measurements were carried out in triplicate. Standard deviations were below 10%. Phg is phenylglycine.

protease.³⁰ At the C-terminus, exchanging norleucine for phenylglycine resulted in a 4-fold enhancement of IC₅₀ at DENV-2 protease. Merging both activity-enhancing fragments provided inhibition of dengue protease in the upper nanomolar range.³¹ A similar range of inhibition at the WNV protease could be achieved by fine-tuning of the nonpolar substituent on the thiazolidinedione scaffold.³² For the sequence (Bz-Arg-Lys-Phg-NH₂), (4-amidino)-L-phenylalanine was found to be a superior mimetic of arginine at dengue protease, resulting in 8-fold higher potency. However, the improvement in activity did not extend to WNV protease.³³

As our initial attempts at C-terminal amino acid modification proved quite rewarding, we decided to further explore and optimize this region through fragment growing, starting from phenylglycine. In parallel, the smaller capping groups at the N-terminus was explored. Optimization at the N-terminus was considered crucial for two reasons: first, to refrain from the previous thiazolidinedione scaffold and its limited capability for the development of potent dual inhibitors; and second, to allow for sufficient structural expansion to extensively probe the binding site around the C-terminal residue, while achieving an optimum balance between molecular size and high antiviral activity in cell culture.

We now report the synthesis and biological evaluation of a new series of dual inhibitors of DENV-2 and WNV proteases comprising substituted benzyl and phenacyl ethers of 4-hydroxyphenylglycine as C-terminal building blocks.

RESULTS AND DISCUSSION

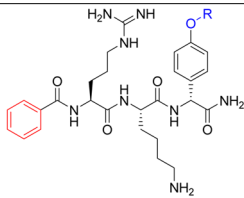
Chemistry. The structures of all target molecules are shown in Tables 1–4. Synthetic routes are outlined in Scheme 1, except for compounds 23–25 and 28–33, which contain alternative peptide sequences. The 4-hydroxyphenylglycine analogues (3a–22a) were obtained by O-alkylation of the commercially available (4-hydroxy)-D-phenylglycine and (4-hydroxy)-L-phenylglycine using appropriately substituted alkyl halogenides according to the procedure first described by Wunsch et al. for O-benzylation of tyrosine.³⁴ The approach involves the formation of a copper complex as a protecting group for the amino acid moiety prior to the alkylation step and was also successfully applied for stereospecific protection of a phenolic hydroxyl group in tyrosine and hydroxyphenylgly-

cine.^{35,36} Briefly, D- or L-(4-hydroxy)-phenylglycine was treated with one equivalent of NaOH, followed by one equivalent of CuSO₄ at 50 °C. This temperature was selected after multiple rounds of optimization and is essential for quantitative complex formation and final product purity. After deprotonation of the hydroxyl group using another equivalent of NaOH, the phenolate of the Cu-complex was alkylated using the respective alkyl bromide, followed by acidification with HCl to release the unprotected 4-hydroxyphenylglycine ethers (3a–9a, 11a, 13a–22a, and 108a) in 32–68% overall yield. For the 4-trifluoromethoxybenzyl and 2-trifluoromethylbenzyl analogues 10a and 12a, the yield was 12% and 20%, respectively, because of the gelatinous nature of the copper-complex that led to loss of material during filtration. The copper complex of 21a was soluble after HCl acidification, and an alternative workup based on copper complexation by 8-quinolinol³⁷ was used instead. All products were obtained in high purity, and no subsequent purification steps were required. As opposed to the traditional strategy for amino acid protection, such as esterification of the carboxylic acid and *N*-Boc formation, the Cu-complex approach requires fewer steps, a simple workup, and no chromatographic purification, rendering it the method of choice for O-alkylation of hydroxyphenylglycine. All hydroxyphenylglycine derivatives were *N*-Fmoc protected using the procedure by Dener et al.³⁸ to give 1, 2, 3b–22b, and 108b, then coupled to Rink amide resin using HATU/DIPEA. Peptide synthesis proceeded according to the Fmoc-protocol as previously described³⁹ until the desired sequence was obtained. A final wash with 25% piperidine in DMF was used for compounds 24 and 25 to cleave any esterification on the unprotected phenolic hydroxyl group.

Structure–Activity Relationships. (SAR). Four series of peptide hybrids (Tables 1–4) were synthesized and evaluated in fluorimetric assays against DENV and WNV proteases and thrombin as a potential off-target. Furthermore, selected compounds were assessed in a HPLC-based DENV or WNV protease assay to exclude false-positive values.

Choice of Sequence. The C-terminal residue modifications recently reported by us revealed steep structure–activity relationships and substantial improvement in activity with Bz-Lys-Arg-Phg-NH₂ (I) showing the highest affinity to DENV protease (IC₅₀ = 3.32 μM). The corresponding D-phenylglycine

Table 2. Inhibitory Activity of *N*-Benzoyl-Capped Tripeptides with the General Structure (Bz-Arg-Lys-X-NH₂), Where X Represents Ethers of (4-Hydroxy)-*D*-phenylglycine as C-Terminal Amino Acid, against DENV and WNV Proteases

| General Structure: | | | | | | | | | | | | | | | |
|--|---|------------------------------------|----------------|------------------------------------|------------------------------------|----------------|------------------------------------|-------|-------|------------------------------------|----------------|------------------------------------|-----|--|--|
|  | | | | | | | | | | | | | | | |
| No. | R | DENV | | | WNV | | | No. | R | DENV | | | WNV | | |
| | | IC ₅₀ (μM) ^a | % ^b | IC ₅₀ (μM) ^c | IC ₅₀ (μM) ^a | % ^b | IC ₅₀ (μM) ^c | | | IC ₅₀ (μM) ^a | % ^b | IC ₅₀ (μM) ^c | | | |
| 27 | | 0.367 | 101.2 | 0.728 | 42 | | 0.321 | 98.1 | 0.406 | | | | | | |
| 34 | | 0.399 | 99.9 | 0.213 | 43 | | 0.186 | 101.6 | 0.321 | | | | | | |
| 35 | | 0.236 | 99.2 | 0.308 | 44 | | 0.151 | 101.0 | 0.493 | | | | | | |
| 36 | | 0.196 | 100.1 | 0.349 | 45 | | 0.177 | 97.8 | 0.615 | | | | | | |
| 37 | | 0.143 | 101.8 | 0.486 | 46 | | 0.147 | 99.0 | 0.804 | | | | | | |
| 38 | | 0.069 | 99.7 | 0.224 | 47 | | 0.309 | 85.2 | n.d. | | | | | | |
| 39 | | 0.182 | 97.1 | n.d. | 48 | | 0.173 | 85.6 | n.d. | | | | | | |
| 40 | | 0.366 | 96.7 | n.d. | 49 | | 0.192 | 92.6 | n.d. | | | | | | |
| 41 | | 0.181 | 97.0 | n.d. | 50 | | 0.486 | 98.8 | 0.508 | | | | | | |
| 109 | | 1.993 | 85.1 | n.d. | | | | | | | | | | | |

^aIC₅₀ values against DEN NS2B-NS3 protease serotype 2 at 50 μM substrate concentration. ^bPercent inhibition of WNV NS2B-NS3 protease (inhibitor 50 μM, substrate 50 μM). ^cIC₅₀ values against WNV NS2B-NS3 protease at 50 μM substrate concentration. n.d. = IC₅₀ was not determined for compounds with less than 98% inhibition. Percent inhibition of thrombin (inhibitor 25 μM, substrate 50 μM) did not exceed 30% (cf. Supporting Information for details). All measurements were carried out in triplicate. Standard deviations were below 10%.

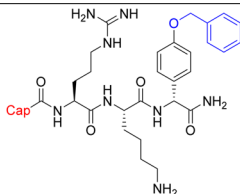
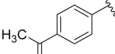
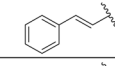
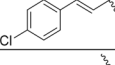
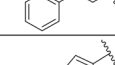
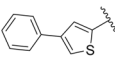
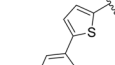
analogue (**23**) was equipotent to the *L*-stereoisomer.³¹ Encouraged by this success, we allocated our research efforts to extensively explore the impact of structural modification of the C-terminal phenylglycine by 4-hydroxy substitution (Table 1). The sequence incorporating (4-hydroxy)-*D*-phenylglycine (**25**) showed slightly higher affinity to DENV protease (IC₅₀ = 2.03 μM). Consequently, this amino acid was then used as an anchor to extend the structure by fragment growth through the metabolically stable ether linkage. Interestingly, *O*-benzylation of **25** to give the first ether **27** led to substantial improvement of inhibitory potency. In comparison to reference **1**, **27** displayed a 9-fold increase in inhibitory potential at DENV protease, in addition to a remarkable enhancement of inhibition at WNV protease by a factor of 80, representing a very promising dual inhibition profile for both targets of interest.

While our earlier findings suggested little contribution of the stereochemistry at the C-terminal position, which we showed for *L*- and *D*-norleucine³¹ and here for *L*- and *D*-phenylglycine (**1** and **23**), this changed with the incorporation of the hydroxyl group, where a clear preference for *D*-configuration could be observed for the hydroxyphenylglycine analogues (**25** vs **24**) and for the corresponding benzyl ethers (**27** vs **26**).

Attempts to shorten the peptidic inhibitors by omitting one basic group in **28** and **29** proved detrimental to the activity at both targets. Switching the position of lysine and arginine in **30** was associated with moderately lower inhibition as opposed to the alternative structure with basic amino acids in *D*-configuration (**31**), which displayed a pronounced loss of activity. To obtain more insight into the orientation of the ether sequence in the binding cavity of both targets, we investigated an interchange of C- and N-terminal residues through the synthesis of sequences **32** and **33**.⁴⁰ Both molecules were far less active than **27**. Docking studies of phenylglycine-containing peptide hybrids on DENV-2^{31,32} and WNV NS2B-NS3³² suggested the positioning of the C-terminal phenylglycine in the S₁ pocket and the N-capping group in S₃ and S₄ pockets for both targets. These findings together with the experimental results suggest an accommodation of the 4-hydroxyphenylglycine ether in the S₁ subsite of the binding cavity in both DENV-2 and WNV proteases, rather than an exchange of its binding location with that of the N-terminal moiety.

Variation of the C-Terminal Ether. After evaluating the peptide sequence, we proceeded to further probe the binding area surrounding the benzyl ether moiety in **27** (Table 2). The diverse choice of ether substituents covered a range of

Table 3. Inhibitory Activity of N-Capped Tripeptides Possessing the General Structure (Cap-Arg-Lys-X-NH₂), X Being the C-Terminal Amino Acid 4-(Benzyloxy)-D-phenylglycine, against DENV and WNV Proteases

| General Structure: | | | | | | | | | |
|--|---|------------------------------------|----------------|------------------------------------|-----|---|------------------------------------|----------------|------------------------------------|
|  | | | | | | | | | |
| No. | N-Cap | DENV | WNV | | No. | N-Cap | DENV | WNV | |
| | | IC ₅₀ (μM) ^a | % ^b | IC ₅₀ (μM) ^c | | | IC ₅₀ (μM) ^a | % ^b | IC ₅₀ (μM) ^c |
| 27 |  | 0.367 | 101.2 | 0.728 | 67 |  | 0.340 | 100.0 | 1.294 |
| 51 |  | 0.262 | 96.4 | n.d. | 68 |  | 0.301 | 98.7 | 0.434 |
| 52 |  | 0.479 | 98.1 | 0.507 | 69 |  | 0.164 | 97.4 | n.d. |
| 53 |  | 0.109 | 98.0 | 0.296 | 70 |  | 0.232 | 83.0 | n.d. |
| 54 |  | 0.179 | 98.2 | 0.490 | 71 |  | 1.039 | 84.6 | n.d. |
| 55 |  | 0.173 | 100.5 | 0.348 | 72 |  | 0.323 | 99.7 | 0.561 |
| 56 |  | 0.099 | 98.8 | 0.158 | 73 |  | 0.721 | 99.4 | 0.368 |
| 57 |  | 0.304 | 97.4 | n.d. | 74 |  | 0.906 | 87.4 | n.d. |
| 58 |  | 0.781 | 95.7 | n.d. | 75 |  | 0.505 | 96.6 | n.d. |
| 59 |  | 0.701 | 96.3 | n.d. | 76 |  | 0.401 | 92.5 | n.d. |
| 60 |  | 0.631 | 98.0 | 0.434 | 77 |  | 0.451 | 97.1 | n.d. |
| 61 |  | 0.805 | 100.3 | 1.661 | 78 |  | 0.194 | 96.2 | n.d. |
| 62 |  | 0.194 | 95.2 | n.d. | 79 |  | 0.375 | 100.0 | 0.430 |
| 63 |  | 0.177 | 98.4 | 0.457 | 80 |  | 0.322 | 94.3 | n.d. |
| 64 |  | 0.364 | 92.6 | n.d. | 81 |  | 0.304 | 98.6 | 0.398 |
| 65 |  | 0.639 | 92.9 | n.d. | 82 |  | 0.347 | 100.0 | 0.360 |
| 66 |  | 0.466 | 95.5 | n.d. | | | | | |

^aIC₅₀ values against DEN NS2B-NS3 protease serotype 2 at 50 μM substrate concentration. ^bPercent inhibition of WNV NS2B-NS3 protease (inhibitor 50 μM, substrate 50 μM). ^cIC₅₀ values against WNV NS2B-NS3 protease at 50 μM substrate concentration. n.d. = IC₅₀ was not determined for compounds with less than 98% inhibition. Percent inhibition of thrombin (inhibitor 25 μM, substrate 50 μM) did not exceed 30% (cf. Supporting Information for details). All measurements were carried out in triplicate. Standard deviations were below 10%.

properties with a focus on hydrophobic groups to counterbalance the high polarity of the basic side chains. Among the benzyl substituted analogues, **109** with a polar electron-

donating amino group in the *para* position had the weakest activity at DENV protease, while **38** with a 4-trifluoromethyl moiety showed the highest inhibitory potential. Exchanging the

trifluoromethyl substituent by the structurally similar trifluoromethoxy group in **39** was associated with loss of potency. Concerning the position of substitution, the ranking of activity goes in the order para > meta > ortho. Extending the ether methylene linker by a carbonyl group in the phenacyl derivative **50** caused a decrease of activity at DENV-2 protease, as opposed to WNV, where it resulted in a slight improvement in inhibitory potential. A more pronounced dissimilarity between the two targets was seen for **34**, which had the highest inhibitory activity at WNV ($IC_{50} = 213$ nM) of this series. It appears that the WNV binding site does not tolerate bulky groups such as *tert*-butyl and naphthyl, with the corresponding analogues (**48** and **49**, respectively) being relatively active at the DENV-2 but not on the WNV protease. For the purpose of dual inhibition, the 4-CF₃-benzyl ether **38** ($IC_{50} = 69$ nM at DENV-2 and 224 nM at WNV) was identified as the most favorable sequence with a 5-fold and 3-fold improvement of potency at DENV-2 and WNV, respectively, in comparison to the unsubstituted parent compound **27**.

Optimization of the N-Terminal Cap. The fine-tuning of the activity at the C-terminal residue was accompanied by a search for an optimal N-terminal cap. This was accomplished by analyzing the inhibitory effect of a diverse collection of small to intermediately sized groups appended to our standard sequence **27** instead of the benzoyl moiety (Table 3). Size restriction in this region was an essential criterion to match the established requirement for activity at the C-terminus, represented by the substituted hydroxyphenylglycine ether scaffold. This would allow for the activity optimization to be less affected by insufficient solubility of the developed inhibitors, a problem that became evident while attempting to incorporate bulkier scaffolds as caps, which moreover caused a decrease of target affinity.

We started our search with bioisosteric replacements of the phenyl ring. For DENV-2, improvement of the inhibition could be seen with pyridine (**51**), thiophene (**53** and **54**), and thiazole (**55–57**), with preferred linkage at position two (**53** and **56**). Cycloalkyl groups generally resulted in lower inhibition; progressive decrease of the ring size (**58–60**) minimally enhanced the activity, with the exception of the cyclopropyl analogue (**61**). With regard to phenyl ring substitution, the *meta*-formyl derivative (**69**) showed the highest potency. Introducing an unsaturated ethylene linker in the *trans*-cinnamic acid analogue (**72**) maintained the activity, whereas the saturated analogue (**74**) was characterized by a nearly 3-fold loss of activity. Thiophene-based annelated rings such as thienothiophenes (**75–76**) or benzothiophene (**77**) were less active than thiophene by a factor of 4 or 5. Ring substitution at the thiophene ring (**79–82**) generated activity in the same range as the benzoyl substituted reference **27**. For both DENV-2 and WNV proteases, the thiazole ring present in **56** ($IC_{50} = 99$ nM at DENV-2 and 158 nM at WNV) and the thiophene scaffold in **53** ($IC_{50} = 109$ nM at DENV-2 and 296 nM at WNV) were the most promising caps for dual inhibition purposes. As already observed for the C-terminal ethers, some discrepancy in the inhibition results could be seen between the two targets. For WNV protease, this was particularly the case for the furan, cyclobutane, and 4-chloro-*trans*-cinnamic acid analogues (**52**, **60**, and **73** respectively), which generated a more pronounced inhibition as opposed to their action on DENV-2 protease. Again, a twice higher potency was observed for the thiophene-substituted derivatives **79**, and **81–82** at

WNV protease, with nearly no improvement at DENV-2 protease.

Fragment Merging. Proteases as targets for drug discovery often encompass distinct subpockets engaging in specific interactions with the side chains of a substrate or a ligand. This makes them attractive examples for the application of fragment-based techniques.^{41,42} Among the various strategies of this approach, our interest has been directed at fragment-growing and fragment-merging.^{43,44} This was first realized by extending the hydroxyphenylglycine sequence **25** to the ethers shown in Table 2. In fragment-merging, we intended to use the activity-optimized fragments with functionalities fitting at different binding positions of the protease targets to generate a series of high affinity inhibitors. For this purpose, selected tripeptides from Tables 2 and 3 were merged, thus incorporating optimal P1 and cap substituents into a single peptidic scaffold. Fragment merging was not limited to the most active sequences. It was also applied to fragments that generated a satisfactory enhancement of *in vitro* potency, while allowing to modulate the lipophilic character of the merged inhibitors, and consequently their membrane permeability needed for higher antiviral effect in cellular assays. In accordance with the concept of the merging strategy, all generated peptide hybrids (Table 4) displayed a higher inhibitory potential than their parent fragments.

The most potent inhibitor **83** was obtained by merging the fragments **38** (4-CF₃-benzyl ether) and **56** (thiazole cap), showing the highest enhancement in inhibitory potency at both DENV and WNV proteases for optimization at the C-terminus and N-terminus, respectively. Indeed, **83** ($IC_{50} = 18$ nM, $K_i = 12$ nM at dengue, $IC_{50} = 50$ nM, $K_i = 39$ nM at WNV) is characterized by a noticeable improvement in binding affinity in comparison to **27** ($IC_{50} = 367$ nM, $K_i = 307$ nM at dengue, $IC_{50} = 728$ nM, $K_i = 536$ nM at WNV) by a factor of 20 at DENV-2 and 14 at WNV. The tripeptide hybrid **83** represents thus the most potent dual inhibitor in this series, followed by **86** ($IC_{50} = 28$ nM, $K_i = 19$ nM at DENV-2, $IC_{50} = 117$ nM, $K_i = 93$ nM at WNV) obtained by combining **38** (4-CF₃-benzyl ether) with **53** (thien-2-yl cap).

Merged molecules inherited the established ranking of the activity and target selectivity linked to their composing entities. All composites maintained an excellent selectivity against thrombin. Generally, compounds showed less inhibition at WNV; this was particularly noticed for sequences with *t*-butyl ethers (**93**, and **95–96**) or annelated caps (**96**, **98–100**, and **102–103**). To confirm this, we determined the inhibitory potential at WNV for the peptide hybrid combining both features (**96**), which, as expected, showed a selectivity factor of 100 between the two proteases. The finding sheds light at differences between both active sites.

Sequences **104–105** and **96** were fluorescent owing to their bithiophene and thienothiophene N-capping moieties as was seen also for peptide **79** (bithiophene cap) and bioisosteric **82** (phenylthiophene cap). Fluorescent compounds were tested in HPLC-based dengue and WNV protease assays to avoid interference with the fluorimetric assays.

Altogether, fragment growing and merging optimization led to a class of tripeptide hybrids which are highly potent dual inhibitors of DENV and WNV proteases. Members of this class have binding affinities in the low nanomolar range without incorporation of highly reactive electrophiles. The most active derivative **83** noticeably outperforms the initial lead **I** ($IC_{50} = 3.32$ μ M, $K_i = 2.12$ μ M at DENV-2, $IC_{50} = 58.10$ μ M, $K_i =$

Table 4. Inhibitory Activity of Merged Sequences against DENV and WNV Proteases

| General Structure: | | | | | |
|--------------------|-------|---|------------------------------------|----------------|------------------------------------|
| | | | | | |
| No. | N-Cap | R | DENV | WNV | |
| | | | IC ₅₀ (μM) ^a | % ^b | IC ₅₀ (μM) ^c |
| 27 | | | 0.367 | 101.2 | 0.728 |
| 83 | | | 0.018 | 100.3 | 0.050 |
| 84 | | | 0.047 | 100.4 | 0.273 |
| 85 | | | 0.050 | 99.1 | 0.166 |
| 86 | | | 0.028 | 101.1 | 0.117 |
| 87 | | | 0.061 | 100.7 | 0.216 |
| 88 | | | 0.068 | 99.3 | 0.231 |
| 89 | | | 0.071 | 99.2 | 0.150 |
| 90 | | | 0.079 | 98.0 | 0.245 |
| 91 | | | 0.148 | 99.4 | 0.487 |
| 92 | | | | 0.111 | 99.6 |
| 93 | | | 0.130 | 91.3 | n.d. |
| 94 | | | 0.120 | 99.3 | 0.821 |
| 95 | | | 0.121 | 85.2 | n.d. |
| 96 | | | 0.157 | 94.1 | 15.92 |
| 97 | | | 0.158 | 99.2 | 0.785 |
| 98 | | | 0.170 | 93.8 | n.d. |
| 99 | | | 0.197 | 97.5 | n.d. |
| 100 | | | 0.203 | 94.2 | n.d. |
| 101 | | | 0.199 | 98.7 | 0.604 |
| 102 | | | 0.243 | 93.1 | n.d. |
| 103 | | | 0.183 | 95.9 | n.d. |
| 104 | | | 0.176 | 100.0 | 0.557 |
| 105 | | | 0.215 | 100.0 | 0.365 |
| 106 | | | 0.129 | 98.0 | 0.221 |

^aIC₅₀ values against DEN NS2B-NS3 protease serotype 2 at 50 μM substrate concentration. ^bPercent inhibition of WNV NS2B-NS3

Table 4. continued

protease (inhibitor 50 μM, substrate 50 μM). ^cIC₅₀ values against WNV NS2B-NS3 protease at 50 μM substrate concentration. n.d. = IC₅₀ was not determined for compounds with less than 98% inhibition except **96**. All measurements were carried out in triplicate. Standard deviations were below 10%.

48.70 μM at WNV) showing 180-fold higher inhibition at dengue and more than a 1000-fold higher activity at WNV.

Selectivity and Binding Mode. To study the potential of the compounds as thrombin inhibitors and determine their selectivity, a screen (25 μM) against thrombin was performed, but no significant inhibition was observed for any compound. A screen of the most promising compounds (Table 4) at 25 μM against trypsin also showed no significant inhibition of this off-target, with the sole exception of **91** (59% inhibition). Complete thrombin and trypsin inhibition data are provided in the Supporting Information.

Tryptophan quenching assays and competition with aprotinin⁴⁵ were used to study the binding mode of selected compounds (**104** and **83**) at the dengue and West Nile virus proteases. The results clearly indicate a binding of the compounds in the active site of the enzymes. Details are given in the Supporting Information. A Cheng–Prusoff plot⁴⁶ for compound **83** at the DENV-2 and WNV proteases revealed a competitive inhibition mechanism (Figure S2).

Docking Studies. Docking studies were performed with AutoDock Vina⁴⁷ using the X-ray structures of DENV-3 NS2B-NS3 (3U1I)⁴⁸ and WNV NS2B-NS3 (2FP7).¹⁰ With the lack of a crystal structure for DENV-2 protease in complex with an inhibitor and considering the high degree of conservation of the binding site between serotypes 2 and 3, the 3U1I structure was considered adequate for docking simulations at DENV. Attempts to dock compounds representing a gradient of activities at the target proteases provided no significant differences in the binding mode. As previously reported,³³ this could be attributed to the high affinity of the present data set, which makes docking simulations unable to determine fine differences in binding that lead to the observed variation of affinity. Considering this aspect and the similarity of our compounds, the binding mode analysis was focused on the most active analogue, compound **83** (Figure 1). In general, the ligand assumed a nearly cyclic orientation in the binding site of either protease. At both DENV and WNV, the obtained binding poses came in agreement with previously reported docking studies from our group,^{31,32} with the phenylglycine ring placed in the S₁ pocket, the arginine in the S₂ pocket, and the N-cap in the S₃ pocket with potential extension to the S₄ pocket in case of larger capping moieties. While these residues did not significantly vary in their orientation in the binding pockets, this was not the case for the lysine side chain, which occupies the space between S₁, S₃, and S₄ pockets, interacting either with the protein or the ligand. The same observation was made before.^{31,32} With respect to the newly introduced benzyl ether, this group was modeled to bind in a previously unexplored binding area between the S₁ and the S₃ pockets. The benzyl ring is placed close to residue 155 (Val155 in DENV-3 or Ile155 in WNV), with the potential for a π–σ interaction between the phenyl ring of the ether and the alkyl side chain of residue 155. This amino acid is conserved in all DENV serotypes and was previously implicated in explaining the lower affinity of aprotinin at WNV protease in comparison

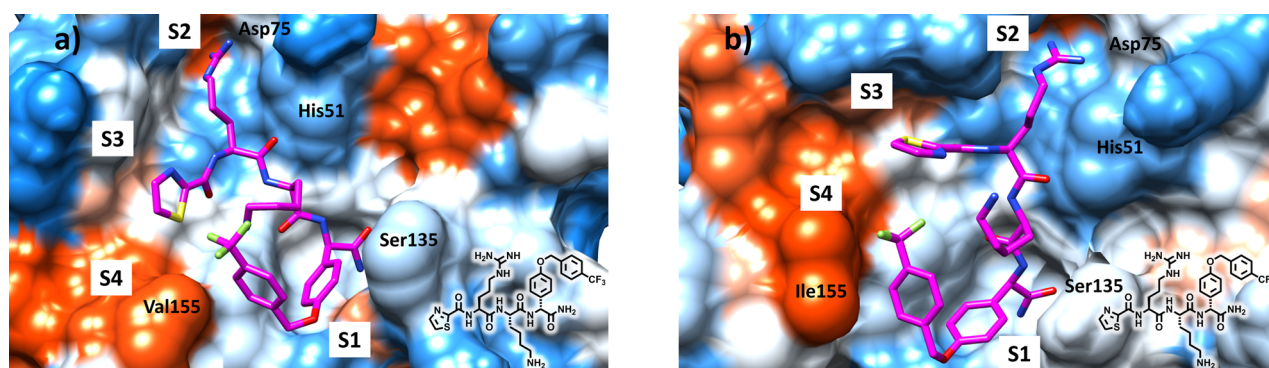


Figure 1. Docking studies of compound **83** at DENV-3 and WNV proteases. The protein surface is colored by amino acid hydrophobicity, with blue indicating hydrophilic and orange indicating hydrophobic regions. The ligand is shown in stick representation. The positions of the specificity pockets, the catalytic triad, and residue 155 are indicated. (a) Docking pose of the ligand–protein complex for DENV protease. (b) Docking pose of the ligand–protein complex for WNV protease.

to DENV protease.⁴⁸ The underlying reason for this difference is the bulkier side chain of isoleucine in WNV as opposed to valine in DENV, which would allow aprotinin to bind deeper in the binding site and create a H-bond interaction with Gly153.⁴⁸ Analogously, this may explain the lower tolerance of the WNV binding site for bulkier benzyl ethers or larger N-terminal caps of the inhibitors presented here.

Antiviral Activity in Cell-Culture and Cytotoxicity Evaluation. To confirm the antiviral effects of the developed tripeptide hybrids on DENV-2 and WNV replication, 12 compounds in addition to our previously reported reference **I**³¹ were chosen for virus titer reduction assays using the Huh-7 human hepatoma cell line infected with DENV-2, and 3 compounds together with the reference **I** were additionally tested in Huh-7 cells infected with WNV.³¹ The selected molecules are characterized by variant protease inhibitory activity, overall size, and lipophilicity. Compounds were first assessed for cytotoxicity by cell viability assays, and the half-maximum cytotoxic concentrations (CC_{50}) were determined (Tables 5 and 6). The viability testing was used to define the upper limit of concentrations for each compound in the plaque assay to eliminate the influence of cytotoxic effects. All selected tripeptides displayed a significant reduction of virus titer and were thus used for EC_{50} determination. Antiviral activity was obtained in a very promising range, with EC_{50} values predominantly between 3 and 20 μM at DENV-2, and between 15 and 23 μM at WNV. Furthermore, the compounds displayed favorable therapeutic indices with the CC_{50} to EC_{50} ratio usually higher than 10. At DENV-2, the most potent compounds **104** and **90** showed EC_{50} values of 3.42 μM and 4.06 μM , respectively, and a promising CC_{50} to EC_{50} ratio (SI (selectivity index) > 25). At WNV, compound **104** displayed the lowest EC_{50} -value of 15.5 μM and a favorable selectivity index (SI > 7).

In contrast to the relatively straightforward SAR discussion of protease inhibition in vitro, analysis of the cellular antiviral activity is complicated by additional aspects, such as membrane permeability and metabolic stability. For DENV-2, antiviral cellular activity of the sequences bearing small aromatic rings at the N-terminus, such as the thiophene-capped **88** and **90**, seem to be sensitive to the lipophilic character of the benzyl ether moiety. As an experimental indicator for lipophilicity, we here consider the retention times (t_R) of the compounds on RP-18 HPLC columns.⁴⁹ For instance, the more lipophilic 3,4-dichlorobenzyl substituted **90** (retention time t_R = 3.22 min)

Table 5. Results of the Dengue Virus Titer Reduction and Viability Assays for Selected Compounds

| General Structure: | | | | | |
|--------------------|----------------------------------|-----------------------------|--------------------|-----------------------------|-----------------------------|
| | | | | | |
| No. | Sequence | IC_{50} (μM) | t_R (min) | EC_{50} (μM) | CC_{50} (μM) |
| I | Bz–Arg–Lys–L–Phg–NH ₂ | 3.323 ³¹ | 2.25 ³¹ | 78.55 ± 3.78 ³³ | > 100 ³³ |
| | Cap | R | | | |
| 27 | | 0.367 | 2.83 | 7.94 ± 2.13 | > 100 |
| 77 | | 0.451 | 3.13 | 20.45 ± 1.44 | > 100 |
| 83 | | 0.018 | 3.11 | 20.35 ± 2.50 | > 100 |
| 86 | | 0.028 | 3.15 | 7.06 ± 0.28 | > 100 |
| 88 | | 0.068 | 2.71 | 54.63 ± 6.55 | > 100 |
| 90 | | 0.079 | 3.22 | 4.06 ± 1.78 | > 100 |
| 93 | | 0.130 | 3.34 | 7.12 ± 3.12 | > 100 |
| 97 | | 0.158 | 3.28 | 5.33 ± 1.19 | 34.34 ± 3.05 |
| 100 | | 0.203 | 3.39 | 10.46 ± 2.70 | 48.54 ± 0.67 |
| 101 | | 0.199 | 3.47 | 7.06 ± 0.60 | 56.75 ± 0.16 |
| 104 | | 0.176 | 3.28 | 3.42 ± 1.30 | > 100 |
| 105 | | 0.215 | 3.60 | 7.60 ± 0.08 | 40.04 ± 1.41 |

showed 14-fold higher anti-DENV effect in cells (EC_{50} = 4.06 μM) than the 3-methoxybenzyl analogue **88** (retention time t_R = 2.71 min; EC_{50} = 54.63 μM), despite having comparable activities in vitro. The lower antiviral activity of the thiazole-capped **83** (EC_{50} = 20.35 μM) compared to the thiophene analogue **86** (EC_{50} = 7.12 μM) could be explained by metabolism in the hepatic Huh-7 cells used for testing, reflecting thus the higher stability of the thiophene ring against

Table 6. Results of the West Nile Virus Titer Reduction and Viability Assays for Selected Compounds

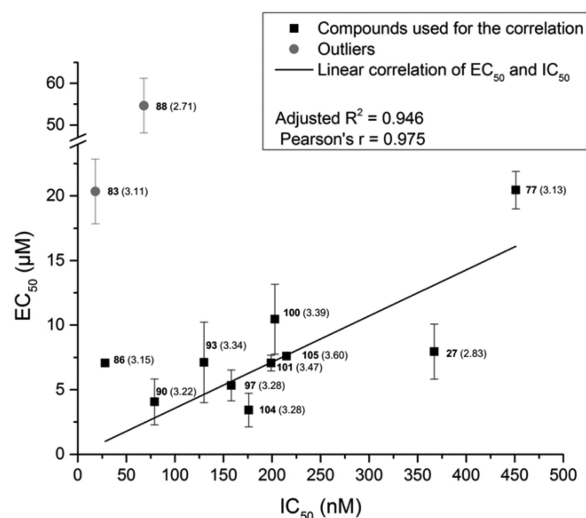
| General Structure: | | | | | |
|--------------------|----------------------------------|-----------------------|----------------------|-----------------------|-----------------------|
| | | | | | |
| No. | Sequence | IC ₅₀ (μM) | t _R (min) | EC ₅₀ (μM) | CC ₅₀ (μM) |
| I | Bz-Arg-Lys-L-Phe-NH ₂ | 58.10 ³¹ | 2.25 ³¹ | > 100 | > 100 |
| | Cap | | | | |
| 83 | | 0.050 | 3.11 | 23.36 ± 3.31 | > 100 |
| 90 | | 0.079 | 3.22 | 23.31 ± 1.21 | > 100 |
| 104 | | 0.557 | 3.28 | 15.55 ± 0.94 | > 100 |

oxidative biotransformation in comparison to thiazole.⁵⁰ Consistent with the obtained results at the isolated DENV-2 and WNV proteases in vitro, the tested compounds were less active at WNV than at DENV-2. Lipophilicity of the inhibitors represented by their retention time (t_R) was found to correlate with the observed antiviral activity. This could be justified by the shorter infection cycle in the WNV assay in comparison to the DENV-2 assay, where factors affecting membrane permeability such as lipophilicity are expected to exert higher influence on the activity of the compounds than metabolic stability. Consequently, compound **104** (retention time t_R = 3.28 min) displayed higher anti-WNV effect in cells (EC_{50} = 15.5 μM) than the slightly more polar derivatives; **83** (retention time t_R = 3.11 min; EC_{50} -value of 23.36 μM) or **90** (retention time t_R = 3.22 min; EC_{50} -value of 23.31 μM).

In an attempt to model the relationship between in vitro and cellular activities, we generated a plot of the antiviral activity on DENV-2 replication in cells (EC_{50} in μM) versus their inhibitory activity on DENV-2 protease (IC_{50} in nM) for the compounds in Table 5 (excluding I). A linear correlation can be obtained with an adjusted R -square of 0.945 and Pearson's r coefficient of 0.975 (Figure 2). However, the variance of activities is relatively small, and therefore any conclusions from this "QSAR" remain limited. In accordance with the discussion above, **88** and **83** were considered as outliers and were not included in the correlation. A certain trend evident from the plot is that inhibition in the plaque assay appears to be related to higher lipophilicity of the inhibitors, which is here expressed as an experimental surrogate (retention time t_R on RP-HPLC).⁴⁹

Taken together, the antiviral activity of this new class of inhibitors is a significant improvement in comparison to the previously published I; a nearly 25-times lower EC_{50} at DENV-2 could be achieved with **104**. Furthermore, for the first time a dual antiviral profile in titer reduction assays was observed, with compound **104** showing at least 7-fold lower EC_{50} at WNV than compound I.

Membrane Permeability and Metabolic Stability. The passive membrane permeability of all compounds tested in DENV-2 or WNV plaque assays (Tables 5 and 6) was further evaluated using the parallel artificial membrane permeability assay (PAMPA).^{51,52} Compounds **27**, **77**, **83**, **86**, **88**, **90**, **97**, **100**, and **101** were not permeable at detectable range, as was previously reported for the reference compound I.³³ The results

**Figure 2.** Correlation between EC_{50} values (μM) from the DENV-2 plaque assay and IC_{50} values (nM) at the DENV-2 NS3-NS2B. The compound t_R (min) is indicated in parentheses.

of the compounds that displayed detectable permeability are listed in Table 7. These include derivatives **93**, **104**, and **105**.

Table 7. Passive Membrane Permeability, Determined by PAMPA, of Selected Compounds

| no. | C_{Acc} (μM) ^a | C_{Don} (μM) ^b | P_e (10 ⁻⁶ cm/s) ^c | R (%) ^d |
|-----|-----------------------------|-----------------------------|--|----------------------|
| 93 | 1.8 ± 0.3 | 197.9 ± 0.1 | 0.33 | 0.44 |
| 104 | 3.4 ± 0.3 | 195.4 ± 0.3 | 0.65 | 1.15 |
| 105 | 4.1 ± 1.3 | 192.3 ± 1.9 | 0.79 | 2.5 |

^aConcentration of the compound in the acceptor plate after 5 h of incubation. ^bConcentration of the compound in the donor plate after 5 h of incubation. ^cPermeability of the compound calculated according to the literature.⁵² ^dMass retention of the compound calculated according to the literature.⁵²

The weak permeability could be linked to the high polarity of the compounds caused by the incorporation of two basic residues. The results of the PAMPA assay may partially explain the difference between the IC_{50} -values at the isolated viral proteases and the EC_{50} values in viral titer reduction assays for DENV-2 and WNV. A slight improvement in passive permeability could be achieved with compounds **93**, **104**, and **105** in comparison to the analogues published previously.³³

Considering the peptidic nature of our inhibitors and their sensitivity to metabolic clearance, particularly hepatic metabolism,⁵³ the metabolic stability of three selected compounds (**83**, **88**, and **104**) was assessed using liver microsomes from rats.³³ Liver microsomes contain phase I metabolic enzymes that perform hydrolysis, reduction, and oxidation of the compounds to generate polar metabolites.⁵⁴ Compounds were chosen with the intention to obtain an understanding of the higher activity of compound **104** in cell-based assays in comparison to analogues such as **83** and **88**, which were more active in vitro at the DENV-2 and WNV proteases. Samples were incubated for 30 min at 37 °C, and the loss of parent compound was monitored. Testosterone was used as the reference compound and showed a half-life time of 63 min. The half-lives of the tested compounds were **83**, 45 min; **88**, 93 min; and **104**, 175 min.

In general, the ether-containing inhibitors displayed a remarkable increase in metabolic stability in comparison to the phenylglycine-based inhibitors (half-life 18–22 min).³³ The improvement in metabolic stability could be attributed to the difference in the C-terminal or P2 residues.

For compound **104**, the improved properties of this derivative with regard to membrane permeability and metabolic stability could provide an explanation for its superior performance in dengue and WNV cell-based assays, in comparison to analogues such as compound **83** that showed higher inhibitory activity in vitro.

CONCLUSIONS

We here report a straightforward approach toward 4-hydroxyphenylglycine ethers as novel non-natural building blocks of compounds with enhanced inhibitory action against the DENV-2 and WNV proteases. The benzoyl-capped benzyl ether analogue **27** showed a promising initial improvement of potency against both target proteases that was achieved by fragment growth from the previously described phenylglycine derivative **1**. The **27** sequence was then optimized through simultaneous C-terminal and N-terminal modifications. On the basis of SAR analysis, selected activity-enhancing fragments were merged to provide a series of highly affine inhibitors. All molecules showed negligible activity on the off-targets thrombin and trypsin. Compounds **83** (thiazole cap, 4-CF₃-benzyl ether), **85** (thiazole cap, 2,6-di-Cl-benzyl ether), **86** (thiophene cap, 4-CF₃-benzyl ether), and **89** (thiophene cap, 4-Br-benzyl ether) displayed a dual inhibition profile at both proteases. However, compounds such as **95** (3-Cl-thiophene cap, 4-*tert*-butyl benzyl ether), **96** (thienothiophene cap, 4-*tert*-butyl benzyl ether), **98** (thienothiophene cap, 4-Cl-benzyl ether), and **102** (benzothiophene cap, 2-CF₃-benzyl ether) were more selective toward dengue protease. The findings provide valuable insight into the molecular recognition preferences of both targets. For the C-terminal ether, small para-substituents such as 4-CF₃ caused effective inhibition of both viral proteases. Bulkier groups, such as 4-*tert*-butyl, were less tolerated at WNV. Small heterocycles as N-capping moieties yielded dual inhibitors whereas annelated caps showed decreased activity at WNV. The effect of the protease inhibitors on viral replication was validated in cellular assays, which showed a reduction of dengue and West Nile virus titers and favorable selectivity indices. The derivative **104** (bithiophene cap, 3-OCH₃-benzyl ether) possessed the highest antiviral activity against DENV-2 and WNV, and displayed an improved permeability and metabolic stability in comparison to those of our previously reported inhibitors. The combination of low-nanomolar in vitro affinities and promising activity in cell culture offers a starting point for future improvements that will be focused on the pharmacokinetic profile of this compound class.

EXPERIMENTAL SECTION

General. The unprotected (4-hydroxy)-D-phenylglycine and (4-hydroxy)-L-phenylglycine, the carboxylic acids used as N-terminal capping groups, and all other chemicals used for synthesis were obtained from Sigma-Aldrich (Germany) and Alfa Aesar, Johnson Matthey (Germany) and were of analytical grade. All solvents were used as obtained from the commercial sources. The protected amino acids were purchased from Orpegen (Germany) and Carbolution Chemicals (Germany). HATU was purchased from Carbolution Chemicals (Germany). The Rink amide resin was purchased from Iris

Biotech (Germany) and was of an average capacity of 0.65 mmol/g. The reaction progress was determined by thin layer chromatography on Merck silica gel plates 60 F254 (UV detection).

NMR spectra were recorded on Varian NMR instruments at 300 or 500 MHz, 300 K in acetone-*d*₆, CDCl₃, CD₃OD, DMSO-*d*₆/NaOD, or D₂O. For the preparation of unprotected amino acid NMR samples in DMSO-*d*₆/NaOD, 0.1 mL of NaOD and 0.5–0.6 mL of DMSO-*d*₆ were added to the amino acid, the mixture was centrifuged to remove undissolved material (if any), and the clear solution was used for NMR analysis. Chemical shifts (δ) are given in parts per million (ppm) in reference to residuals of nondeuterated solvents as internal standard. (¹H NMR: acetone-*d*₆ δ = 2.05 ppm, CDCl₃ δ = 7.26 ppm, CD₃OD: δ = 4.87 ppm, DMSO-*d*₆ δ = 2.50 ppm, D₂O: δ = 4.79 ppm. ¹³C NMR (APT): acetone-*d*₆ δ = 29.84 ppm, CDCl₃ δ = 77.16 ppm, CD₃OD: δ = 49.00 ppm, DMSO-*d*₆ δ = 39.52 ppm.) Coupling constants (*J*) are given in hertz (Hz). Multiplicity is reported as s (singlet), d (doublet), t (triplet), dd (doublet of doublet), td (triplet of doublet), and m (multiplet).

HR-ESI mass spectra were measured on a Bruker microTOF-Q II instrument. All tested target compounds were obtained with a purity of at least 95%, unless otherwise indicated. Analysis was carried out using 50 μ M samples in water/acetonitrile (1:1). Purity of the peptide hybrids was determined by HPLC on a Jasco HPLC system with a DAD detector on an RP-18 column (ReproSil-Pur-ODS-3, Dr. Maisch GmbH, Germany, 5 μ m, 50 mm \times 2 mm) using method A. Purity of DENV and WNV FRET (Förster (fluorescence) resonance energy transfer) substrates was determined by LC-MS analysis carried out using an Agilent HPLC system with MWD detector combined with the Bruker microTOF-Q II instrument on a RP-18 column (ReproSil-Pur-ODS-3, Dr. Maisch GmbH, Germany, 5 μ m, 50 mm \times 2 mm) using method B. The conditions used for method A were as follows: water (0.1% TFA); eluent B, acetonitrile (0.1% TFA); injection volume, 10 μ L; flow rate, 1 mL/min; and gradient, 1% B (0.2 min), 100% B (7 min), 100% B (8 min), 1% B (8.1 min), and 1% B (10 min). UV-detection was performed at 254 nm. The conditions used for method B were as follows: water (0.1% HCO₂H); eluent B, acetonitrile (0.1% HCO₂H); injection volume, 10 μ L; flow rate, 0.4 mL/min; and gradient, 5% B (1 min), 95% B (10 min), 5% B (10.1 min), and 5% B (12 min). UV-detection was performed at 214, 254, and 280 nm. Chromatograms recorded at 254 nm were used for purity assessment.

General Procedure for the Synthesis of (4-Hydroxy)-phenylglycine Ethers. A solution of the amino acid (1 equiv) in 1 M NaOH (1 equiv) and a solution of CuSO₄·5H₂O (0.67 equiv) in water (10 mL) were warmed to 50 °C under stirring. Both solutions were combined, and the reaction mixture was stirred for 30 min at 50 °C. After cooling on an ice–water bath, the blue precipitate of the amino acid Cu-complex separated immediately. The precipitate was isolated, washed with water, and dried. The Cu-complex was dissolved in methanol (25 mL) and 1 M NaOH (1 equiv). The corresponding benzyl or phenacyl bromide (1.1 equiv) was added, and the mixture was stirred at room temperature overnight. The insoluble Cu-complex of the resulting ether was collected by filtration, washed with MeOH, and then with water to remove excess of the unreacted starting material. Finally, 1 M HCl (2 equiv) was added to release the product from the Cu-complex. The precipitated product was washed with water and dried under reduced pressure.³⁴ The crude product was used for subsequent synthetic steps without further purification. An alternative workup using 8-quinolinol³⁷ was employed to obtain **21a** due to the solubility of the Cu-product complex after acidification. To the resulting solution, 8-hydroxyquinoline (0.5 equiv) in acetone was added, and the mixture was stirred at room temperature for 3 h. The solution was alkalinized with 1 M NaOH, and the green precipitate of copper 8-hydroxyquinolate was removed by filtration. Acetone was evaporated under reduced pressure, and the solution was acidified using 1 M HCl. After lyophilization, the solid was dissolved in EtOH/ACN (1:1) to allow the removal of the insoluble NaCl by filtration. The solvent was evaporated to afford the amino acid product, without further purification.

(4-Benzyloxy)-L-phenylglycine (3a). Compound **3a** was obtained according to the general procedure from (4-hydroxy)-L-phenylglycine (1003 mg, 6 mmol) and benzyl bromide (0.78 mL, 6.6 mmol) as a beige solid (920 mg, 52% yield). ^1H NMR (300 MHz, DMSO- d_6 /NaOD) δ 7.54–7.38 (m, 5H), 7.32 (d, J = 8.7 Hz, 2H), 7.04 (d, J = 8.8 Hz, 2H), 5.15 (s, 2H), 4.31 (s, 1H); ^{13}C NMR (75 MHz, DMSO- d_6 /NaOD) δ 179.64, 155.48, 134.95, 133.75, 127.22, 126.82, 126.55, 126.53, 113.75, 113.75, 68.76, 58.22. HRMS (ESI): m/z [M – H] $^-$ calcd for C₁₅H₁₄NO₃, 256.0979; found, 256.0973.

(4-Benzyloxy)-D-phenylglycine (4a). Compound **4a** was obtained according to the general procedure from (4-hydroxy)-D-phenylglycine (1003 mg, 6 mmol) and benzyl bromide (0.78 mL, 6.6 mmol) as a beige solid (920 mg, 52% yield). ^1H NMR (300 MHz, D₂O/NaOD) δ 7.45–7.29 (m, 5H), 7.26 (d, J = 8.6 Hz, 2H), 6.83 (d, J = 8.7 Hz, 2H), 5.04 (s, 2H), 3.94 (s, 1H); ^{13}C NMR (APT, 75 MHz, DMSO- d_6 /NaOD) δ 176.45, 156.54, 138.77, 137.55, 128.53, 127.84, 127.81, 127.64, 113.90, 69.22, 60.22. HRMS (ESI): m/z [M – H] $^-$ calcd for C₁₅H₁₄NO₃, 256.0979; found, 256.0973.

[4-(4-Cyano)benzyloxy]-D-phenylglycine (5a). Compound **5a** was obtained according to the general procedure from (4-hydroxy)-D-phenylglycine (502 mg, 3 mmol) and 4-bromomethyl benzonitrile (0.60 mL, 3.3 mmol) as a beige solid (600 mg, 63% yield). ^1H NMR (300 MHz, DMSO- d_6 /NaOD) δ 7.83 (d, J = 8.5 Hz, 2H), 7.61 (d, J = 8.4 Hz, 2H), 7.27 (d, J = 8.6 Hz, 2H), 6.83 (d, J = 8.7 Hz, 2H), 3.95 (s, 2H), 3.74 (s, 1H). ^{13}C NMR (APT, 75 MHz, DMSO- d_6 /NaOD) δ 176.62, 156.19, 143.43, 139.01, 132.54, 128.16, 127.98, 127.91, 127.05, 118.99, 117.92, 113.98, 110.47, 70.21, 60.24. HRMS (ESI): m/z [M – H] $^-$ calcd for C₁₆H₁₃N₂O₃, 281.0932; found, 281.0939.

[4-(4-Bromo)benzyloxy]-D-phenylglycine (6a). Compound **6a** was obtained according to the general procedure from (4-hydroxy)-D-phenylglycine (502 mg, 3 mmol) and 4-bromobenzyl bromide (825 mg, 3.3 mmol) as a light brown solid (726 mg, 65% yield). ^1H NMR (300 MHz, DMSO- d_6 /NaOD) δ 7.56 (d, J = 8.1 Hz, 3H), 7.38 (d, J = 8.2 Hz, 2H), 7.24 (d, J = 7.5 Hz, 1H), 6.94–6.82 (m, 2H), 5.15 (s, 1H), 5.05 (s, 2H). ^{13}C NMR (APT, 75 MHz, DMSO- d_6 /NaOD) δ 175.69, 153.67, 137.10, 135.15, 131.48, 129.80, 120.89, 68.52, 57.64. HRMS (ESI): m/z [M – H] $^-$ calcd for C₁₅H₁₃BrNO₃, 334.0084; found, 334.0063.

[4-(4-Fluoro)benzyloxy]-D-phenylglycine (7a). Compound **7a** was obtained according to the general procedure from (4-hydroxy)-D-phenylglycine (502 mg, 3 mmol) and 4-fluorobenzyl bromide (0.41 mL, 3.3 mmol) as a beige solid (500 mg, 53% yield). ^1H NMR (300 MHz, DMSO- d_6 /NaOD) δ 7.46 (dd, J = 8.6, 5.7 Hz, 2H), 7.26 (d, J = 8.6 Hz, 2H), 7.22–7.12 (m, 2H), 6.83 (d, J = 8.7 Hz, 2H), 5.02 (s, 2H), 3.94 (s, 1H). ^{13}C NMR (because of the coupling with the fluorine atom, some of the split signals in ^{13}C NMR (APT) of fluorinated amino acids could not be detected) (APT, 75 MHz, DMSO- d_6 /NaOD) δ 176.49, 156.52, 138.81, 133.86, 129.96 (d, J = 8.2 Hz), 127.95 (d, J = 1.4 Hz), 115.41 (d, J = 21.3 Hz), 114.03, 68.61, 60.30. HRMS (ESI): m/z [M – H] $^-$ calcd for C₁₅H₁₃FNO₃, 274.0885; found, 274.0888.

[4-(4-Chloro)benzyloxy]-D-phenylglycine (8a). Compound **8a** was obtained according to the general procedure from (4-hydroxy)-D-phenylglycine (1003 mg, 6 mmol) and 4-chlorobenzyl bromide (1356 mg, 6.6 mmol) as a light brown solid (1000 mg, 51% yield). ^1H NMR (300 MHz, DMSO- d_6 /NaOD) δ 7.48–7.39 (m, 4H), 7.25 (d, J = 8.5 Hz, 2H), 6.82 (d, J = 8.7 Hz, 2H), 5.05 (s, 2H), 3.90 (s, 1H). ^{13}C NMR (APT, 75 MHz, DMSO- d_6 /NaOD) δ 171.01, 156.21, 136.63, 132.27, 129.40, 128.47, 127.80, 113.82, 68.36, 60.26. HRMS (ESI): m/z [M – H] $^-$ calcd for C₁₅H₁₃ClNO₃, 290.0589; found, 290.0589.

[4-(4-Trifluoromethyl)benzyloxy]-D-phenylglycine (9a). Compound **9a** was obtained according to the general procedure from (4-hydroxy)-D-phenylglycine (502 mg, 3 mmol) and 4-(trifluoromethyl)benzyl bromide (0.51 mL, 3.3 mmol) as a beige solid (320 mg, 30% yield). ^1H NMR (300 MHz, DMSO- d_6 /NaOD) δ 7.73 (d, J = 8.1 Hz, 2H), 7.64 (d, J = 8.0 Hz, 2H), 7.26 (d, J = 8.6 Hz, 2H), 6.84 (d, J = 8.7 Hz, 2H), 3.94 (s, 1H), 3.53 (s, 2H). ^{13}C NMR (because of the coupling with the fluorine atom, some of the split signals in ^{13}C NMR (APT) of fluorinated amino acids could not be detected) (APT, 75 MHz, DMSO- d_6 /NaOD) δ 176.43, 156.29, 142.44, 138.96, 129.27,

128.36 (d, J = 32.3 Hz), 128.08, 128.06, 127.97, 126.22 (d, J = 1.5 Hz), 125.47 (d, J = 3.8 Hz), 122.62, 113.98, 68.34, 60.24. HRMS (ESI): m/z [M – H] $^-$ calcd for C₁₆H₁₃F₃NO₃, 324.0853; found, 324.0853.

[4-(4-Trifluoromethoxy)benzyloxy]-D-phenylglycine (10a). Compound **10a** was obtained according to the general procedure from (4-hydroxy)-D-phenylglycine (502 mg, 3 mmol) and 4-(trifluoromethoxy)benzyl bromide (0.58 mL, 3.3 mmol) as a beige solid (131 mg, 12% yield). ^1H NMR (300 MHz, DMSO- d_6 /NaOD) δ 7.55 (d, J = 8.6 Hz, 2H), 7.36 (d, J = 8.0 Hz, 2H), 7.26 (d, J = 8.6 Hz, 2H), 6.83 (d, J = 8.6 Hz, 2H), 5.08 (s, 2H), 3.92 (s, 1H). ^{13}C NMR (because of the coupling with the fluorine atom, some of the split signals in ^{13}C NMR (APT) of fluorinated amino acids could not be detected) (APT, 75 MHz, DMSO- d_6 /NaOD) δ 176.11, 156.41, 142.85, 140.07, 139.05, 137.17, 133.97, 129.56, 127.96, 121.22, 113.96, 68.38, 60.33. HRMS (ESI): m/z [M – H] $^-$ calcd for C₁₆H₁₃F₃NO₄, 340.0802; found, 340.0801.

[4-(2-Bromo)benzyloxy]-D-phenylglycine (11a). Compound **11a** was obtained according to the general procedure from (4-hydroxy)-D-phenylglycine (1003 mg, 6 mmol) and 2-bromobenzyl bromide (1800 mg, 6.6 mmol) as a beige solid (1250 mg, 56% yield). ^1H NMR (300 MHz, DMSO- d_6 /NaOD) δ 7.65 (dd, J = 7.9, 1.1 Hz, 1H), 7.54 (dd, J = 7.6, 1.6 Hz, 1H), 7.40 (td, J = 7.5, 1.2 Hz, 1H), 7.34–7.24 (m, 3H), 6.84 (d, J = 8.7 Hz, 2H), 5.06 (s, 2H), 3.95 (s, 1H). ^{13}C NMR (APT, 75 MHz, DMSO- d_6 /NaOD) δ 176.50, 156.50, 139.04, 136.36, 136.31, 132.82, 130.36, 130.26, 128.14, 128.04, 122.94, 113.95, 69.27, 60.31. HRMS (ESI): m/z [M – H] $^-$ calcd for C₁₅H₁₃BrNO₃, 334.0084; found, 334.0083.

[4-(2-Trifluoromethyl)benzyloxy]-D-phenylglycine (12a). Compound **12a** was obtained according to the general procedure from (4-hydroxy)-D-phenylglycine (2006 mg, 12 mmol) and 2-(trifluoromethyl)benzyl bromide (2.01 mL, 13.2 mmol) as a beige solid (850 mg, 20% yield). ^1H NMR (300 MHz, DMSO- d_6 /NaOD) δ 7.77 (d, J = 7.8 Hz, 1H), 7.73–7.65 (m, 2H), 7.59–7.52 (m, 1H), 7.27 (d, J = 8.7 Hz, 2H), 6.82 (d, J = 8.7 Hz, 2H), 3.95 (s, 2H), 3.55 (s, 1H). ^{13}C NMR (because of the coupling with the fluorine atom, some of the split signals in ^{13}C NMR (APT) of fluorinated amino acids could not be detected) (APT, 75 MHz, DMSO- d_6 /NaOD) δ 176.53, 156.37, 139.10, 135.39 (d, J = 1.8 Hz), 133.03, 130.50, 128.85, 128.06, 127.00 (d, J = 30.4 Hz), 126.37, 126.35, 126.27, 126.20, 122.74, 113.90, 71.92 (d, J = 1.0 Hz), 60.28. HRMS (ESI): m/z [M – H] $^-$ calcd for C₁₆H₁₃F₃NO₃, 324.0853; found, 324.0869.

[4-(2-Chloro)benzyloxy]-D-phenylglycine (13a). Compound **13a** was obtained according to the general procedure from (4-hydroxy)-D-phenylglycine (1003 mg, 6 mmol) and 2-chlorobenzyl bromide (0.86 mL, 6.6 mmol) as a beige solid (960 mg, 49% yield). ^1H NMR (300 MHz, DMSO- d_6 /NaOD) δ 7.59–7.53 (m, 1H), 7.51–7.45 (m, 1H), 7.40–7.33 (m, 2H), 7.28 (d, J = 8.6 Hz, 2H), 6.84 (d, J = 8.7 Hz, 2H), 5.10 (s, 2H), 3.95 (s, 1H). ^{13}C NMR (APT, 75 MHz, DMSO- d_6 /NaOD) δ 176.41, 156.45, 139.09, 134.77, 132.67, 130.22, 130.18, 129.93, 129.54, 127.99, 127.54, 113.89, 67.00, 60.28. HRMS (ESI): m/z [M – H] $^-$ calcd for C₁₅H₁₃ClNO₃, 290.0589; found, 290.0596.

[4-(3-Chloro)benzyloxy]-D-phenylglycine (14a). Compound **14a** was obtained according to the general procedure from (4-hydroxy)-D-phenylglycine (1003 mg, 6 mmol) and 3-chlorobenzyl bromide (0.87 mL, 6.6 mmol) as a beige solid (880 mg, 45% yield). ^1H NMR (300 MHz, DMSO- d_6 /NaOD) δ 7.47 (s, 1H), 7.41–7.32 (m, 3H), 7.26 (d, J = 8.6 Hz, 2H), 6.83 (d, J = 8.7 Hz, 2H), 5.06 (s, 2H), 3.93 (s, 1H). ^{13}C NMR (APT, 75 MHz, DMSO- d_6 /NaOD) δ 176.41, 156.38, 140.30, 138.97, 133.30, 130.60, 127.99, 127.82, 127.29, 126.22, 114.03, 68.40, 60.31. HRMS (ESI): m/z [M – H] $^-$ calcd for C₁₅H₁₃ClNO₃, 290.0589; found, 290.0588.

[4-(2,6-Dichloro)benzyloxy]-D-phenylglycine (15a). Compound **15a** was obtained according to the general procedure from (4-hydroxy)-D-phenylglycine (1003 mg, 6 mmol) and 2,6-dichlorobenzyl bromide (1583 mg, 6.6 mmol) as a beige solid (700 mg, 32% yield). ^1H NMR (300 MHz, DMSO- d_6 /NaOD) δ 7.57–7.52 (m, 2H), 7.48–7.40 (m, 1H), 7.30 (d, J = 8.6 Hz, 2H), 6.88 (d, J = 8.7 Hz, 2H), 5.17 (s, 2H), 3.95 (s, 1H). ^{13}C NMR (APT, 75 MHz, DMSO- d_6 /NaOD) δ 176.83, 156.71, 139.42, 136.12, 132.07, 131.56, 128.86, 127.89, 113.65,

64.99, 60.25. HRMS (ESI): m/z $[M - H]^-$ calcd for $C_{15}H_{12}Cl_2NO_3$, 324.0200; found, 324.0208.

[4-(3,4-Dichlorobenzoyloxy)-D-phenylglycine (16a)]. Compound 16a was obtained according to the general procedure from (4-hydroxy)-D-phenylglycine (502 mg, 3 mmol) and 3,4-dichlorobenzyl bromide (0.48 mL, 3.3 mmol) as a beige solid (490 mg, 45% yield). 1H NMR (300 MHz, DMSO- d_6 /NaOD) δ 7.68 (d, $J = 1.7$ Hz, 1H), 7.63 (d, $J = 8.3$ Hz, 1H), 7.42 (dd, $J = 8.3, 1.9$ Hz, 1H), 7.26 (d, $J = 8.6$ Hz, 2H), 6.83 (d, $J = 8.6$ Hz, 2H), 5.06 (d, $J = 6.1$ Hz, 1H), 3.92 (s, 1H). ^{13}C NMR (APT, 75 MHz, DMSO- d_6 /NaOD) δ 176.40, 156.42, 136.11, 131.15, 130.76, 129.40, 127.87, 127.85, 127.84, 113.87, 70.92, 60.23. HRMS (ESI): m/z $[M - H]^-$ calcd for $C_{15}H_{12}Cl_2NO_3$, 324.0200; found, 324.0207.

[4-(3-Methoxybenzoyloxy)-D-phenylglycine (17a)]. Compound 17a was obtained according to the general procedure from (4-hydroxy)-D-phenylglycine (1003 mg, 6 mmol) and 3-methoxybenzyl chloride (0.92 mL, 6.6 mmol) as a light brown solid (930 mg, 48% yield). 1H NMR (300 MHz, DMSO- d_6 /NaOD) δ 7.33–7.20 (m, 2H), 6.99 (d, $J = 7.8$ Hz, 2H), 6.95–6.77 (m, 4H), 5.04 (s, 1H), 3.74 (s, 3H), 3.46 (s, 2H). ^{13}C NMR (APT, 75 MHz, DMSO- d_6 /NaOD) δ 172.68, 159.42, 151.36, 139.20, 129.65, 128.11, 126.79, 126.17, 119.67, 116.50, 113.18, 113.05, 69.11, 59.71, 55.15. HRMS (ESI): m/z $[M - H]^-$ calcd for $C_{16}H_{16}NO_4$, 286.1085; found, 286.1062.

[4-(3-Methylbenzoyloxy)-D-phenylglycine (18a)]. Compound 18a was obtained according to the general procedure from (4-hydroxy)-D-phenylglycine (1504 mg, 9 mmol) and 3-methylbenzyl bromide (1.34 mL, 9.9 mmol) as a beige solid (1680 mg, 61% yield). 1H NMR (300 MHz, DMSO- d_6 /NaOD) δ 7.28–7.16 (m, 5H), 7.10 (d, $J = 7.1$ Hz, 1H), 6.82 (d, $J = 8.7$ Hz, 2H), 4.99 (s, 2H), 3.93 (s, 1H), 2.30 (s, 3H). ^{13}C NMR (APT, 75 MHz, DMSO- d_6 /NaOD) δ 176.40, 156.68, 138.72, 137.79, 137.54, 128.53, 128.27, 127.92, 124.82, 113.97, 69.35, 60.30, 21.20. HRMS (ESI): m/z $[M - H]^-$ calcd for $C_{16}H_{16}NO_3$, 270.1136; found, 270.1132.

[4-(4-tert-Butylbenzoyloxy)-D-phenylglycine (19a)]. Compound 19a was obtained according to the general procedure from (4-hydroxy)-D-phenylglycine (2006 mg, 12 mmol) and 4-tert-butylbenzyl bromide (2.65 mL, 13.2 mmol) as a beige solid (2100 mg, 50% yield). 1H NMR (300 MHz, DMSO- d_6 /NaOD) δ 7.38 (d, $J = 8.5$ Hz, 2H), 7.33 (d, $J = 8.5$ Hz, 2H), 7.24 (d, $J = 8.6$ Hz, 2H), 6.81 (d, $J = 8.7$ Hz, 2H), 5.00 (s, 2H), 3.93 (s, 1H), 1.26 (s, 9H). ^{13}C NMR (APT, 75 MHz, DMSO- d_6 /NaOD) δ 176.52, 156.70, 150.40, 138.60, 134.61, 127.94, 127.66, 125.38, 113.97, 69.09, 60.31, 34.48, 31.35. HRMS (ESI): m/z $[M - H]^-$ calcd for $C_{19}H_{22}NO_3$, 312.1605; found, 312.1606.

[4-(Naphth-2-yl)methoxy]-D-phenylglycine (20a)]. Compound 20a was obtained according to the general procedure from (4-hydroxy)-D-phenylglycine (1003 mg, 6 mmol) and 2-bromomethyl naphthalene (1460 mg, 6.6 mmol) as a light yellow solid (1400 mg, 68% yield). 1H NMR (300 MHz, DMSO- d_6 /NaOD) δ 7.97–7.87 (m, 4H), 7.55 (dd, $J = 8.4, 1.7$ Hz, 1H), 7.52–7.48 (m, 2H), 7.26 (d, $J = 8.4$ Hz, 2H), 6.88 (d, $J = 8.7$ Hz, 2H), 5.22 (s, 2H), 3.93 (s, 1H). ^{13}C NMR (APT, 75 MHz, DMSO- d_6 /NaOD) δ 176.34, 156.67, 138.87, 135.29, 132.99, 132.69, 128.26, 127.98, 127.96, 127.81, 126.53, 126.29, 126.24, 125.84, 114.10, 69.49, 60.33. HRMS (ESI): m/z $[M - H]^-$ calcd for $C_{19}H_{16}NO_3$, 306.1136; found, 306.1131.

[4-Phenacyloxy)-D-phenylglycine (21a)]. Compound 21a was obtained according to the general procedure from (4-hydroxy)-D-phenylglycine (502 mg, 3 mmol) and 2-bromoacetophenone (657 mg, 3.3 mmol) as a brown solid (484 mg, 50% yield). 1H NMR (300 MHz, DMSO- d_6 /NaOD) δ 7.93–7.78 (m, 2H), 7.36 (dd, $J = 8.2, 1.2$ Hz, 1H), 7.29–7.17 (m, 2H), 6.72 (d, $J = 8.5$ Hz, 2H), 6.04 (d, $J = 8.4$ Hz, 2H), 4.45 (s, 1H), 3.74 (s, 2H). ^{13}C NMR (APT, 75 MHz, DMSO- d_6 /NaOD) δ 200.37, 178.70, 169.42, 131.18, 130.03, 129.11, 128.77, 127.21, 127.19, 126.34, 126.32, 125.71, 117.84, 73.81, 60.80. HRMS (ESI): m/z $[M - H]^-$ calcd for $C_{16}H_{14}NO_4$, 284.0928; found, 284.0929.

[4-(4-Bromo)phenacyloxy)-D-phenylglycine (22a)]. Compound 22a was obtained according to the general procedure from (4-hydroxy)-D-phenylglycine (1003 mg, 6 mmol) and 2,4'-dibromoacetophenone (2001 mg, 6.6 mmol) as a yellow solid (900 mg, 37%

yield). 1H NMR (300 MHz, DMSO- d_6 /NaOD) δ 7.56 (d, $J = 8.5$ Hz, 2H), 7.30 (d, $J = 8.5$ Hz, 2H), 7.21 (d, $J = 8.6$ Hz, 2H), 6.89 (d, $J = 8.6$ Hz, 2H), 3.95 (s, 2H), 3.74 (s, 1H). ^{13}C NMR (APT, 75 MHz, DMSO- d_6 /NaOD) δ 204.39, 173.99, 157.78, 133.50, 131.38, 130.18, 129.93, 127.46, 127.25, 126.81, 117.90, 114.31, 73.22, 60.34. HRMS (ESI): m/z $[M - H]^-$ calcd for $C_{16}H_{13}BrNO_4$, 362.0033; found, 362.0022.

N_ϵ -Boc-[4-(4-amino)benzoyloxy]-D-phenylglycine (108a)]. Compound 108a was obtained according to the general procedure from (4-hydroxy)-D-phenylglycine (251 mg, 1.5 mmol) and 107b (the synthesis is described in the Supporting Information) (472 mg, 1.65 mmol) as a yellow solid (200 mg, 33% yield). 1H NMR (300 MHz, DMSO- d_6 /NaOD) δ 7.22 (d, $J = 8.6$ Hz, 2H), 7.18 (d, $J = 8.5$ Hz, 2H), 6.97 (d, $J = 8.5$ Hz, 2H), 6.79 (d, $J = 8.7$ Hz, 2H), 4.79 (s, 2H), 3.94 (s, 1H), 1.32 (s, 9H). ^{13}C NMR (APT, 75 MHz, DMSO- d_6 /NaOD) δ 176.60, 156.76, 138.00, 128.01, 127.62, 120.45, 113.81, 74.90, 69.74, 60.05, 28.74. HRMS (ESI): m/z $[M - H]^-$ calcd for $C_{20}H_{13}N_2O_5$, 371.1612; found, 371.1614.

General Procedure for the Synthesis of N_α -Fmoc-Protected Amino Acids. A solution of the amino acid or its hydrochloride salt (1 equiv) and DIPEA (2–3 equiv) in 20 mL of acetonitrile/water (1:1) is stirred at room temperature for 20 min, then Fmoc-OSu (0.9–0.95 equiv) is added. After 30 min, most of the solids have dissolved. The reaction progress was monitored for the disappearance of Fmoc-OSu by TLC (solvent system: ethyl acetate). When the reaction was completed (1.5–2h), the solution was acidified to pH 2 using 1 M aqueous HCl, 10 mL of water were added, and the mixture was allowed to stir for an additional hour. Finally, the resulting precipitate was collected by filtration, washed with water, dried under reduced pressure, and used as crude product without further purification for solid phase peptide synthesis.³⁸

N_α -Fmoc-(4-hydroxy)-L-phenylglycine (1). Following the general procedure, 4-(hydroxy)-L-phenylglycine (668 mg, 4 mmol), DIPEA (1.39 mL, 8 mmol), and Fmoc-OSu (1.21 g, 3.6 mmol) were reacted together to give 1 as a white solid (950 mg, 68% yield). 1H NMR (300 MHz, acetone- d_6) δ 7.85 (d, $J = 7.5$ Hz, 2H), 7.73 (d, $J = 7.3$ Hz, 2H), 7.40 (t, $J = 7.4$ Hz, 2H), 7.35–7.27 (m, 4H), 7.09 (d, $J = 7.5$ Hz, 1H), 6.85 (d, $J = 8.6$ Hz, 2H), 5.26 (d, $J = 7.6$ Hz, 1H), 4.38–4.28 (m, 2H), 4.26–4.19 (m, 1H). HRMS (ESI): m/z $[M - H]^-$ calcd for $C_{23}H_{18}NO_5$, 388.1190; found, 388.1185.

N_α -Fmoc-(4-hydroxy)-D-phenylglycine (2). Following the general procedure, 4-(hydroxy)-D-phenylglycine (668 mg, 4 mmol), DIPEA (1.39 mL, 8 mmol), and Fmoc-OSu (1214 mg, 3.6 mmol) were reacted together to give 2 as a white solid (1000 mg, 72% yield). 1H NMR (300 MHz, acetone) δ 7.85 (d, $J = 7.5$ Hz, 2H), 7.73 (d, $J = 7.4$ Hz, 2H), 7.40 (t, $J = 7.4$ Hz, 2H), 7.36–7.24 (m, 4H), 7.10 (d, $J = 7.5$ Hz, 1H), 6.85 (d, $J = 8.6$ Hz, 2H), 6.37 (s, 1H), 5.27 (d, $J = 7.7$ Hz, 1H), 4.40–4.28 (m, 2H), 4.28–4.17 (m, 1H); ^{13}C NMR (75 MHz, acetone) δ 172.65, 158.30, 156.57, 156.55, 145.09, 144.98, 129.82, 128.50, 127.94, 126.23, 126.18, 120.77, 116.22, 67.37, 58.45, 47.96. HRMS (ESI): m/z $[M - H]^-$ calcd for $C_{23}H_{18}NO_5$, 388.1190; found, 388.1196.

N_α -Fmoc-(4-benzoyloxy)-L-phenylglycine (3b). Following the general procedure, 3a (588 mg, 2 mmol), DIPEA (1.05 mL, 6 mmol), and Fmoc-OSu (607 mg, 1.8 mmol) were reacted together to give 3b as a beige solid (750 mg, 87% yield). 1H NMR (300 MHz, $CDCl_3$) δ 7.74 (d, $J = 8.8$ Hz, 3H), 7.57 (d, $J = 7.0$ Hz, 1H), 7.42–7.30 (m, 9H), 7.17 (s, 2H), 6.95 (d, $J = 8.7$ Hz, 2H), 5.74 (d, $J = 6.6$ Hz, 1H), 5.35 (d, $J = 6.7$ Hz, 1H), 5.05 (s, 2H), 4.37 (d, $J = 6.5$ Hz, 2H), 4.25–4.15 (m, 1H). HRMS (ESI): m/z $[M - H]^-$ calcd for $C_{30}H_{24}NO_5$, 478.1660; found, 478.1645.

N_α -Fmoc-(4-benzoyloxy)-D-phenylglycine (4b). Following the general procedure, 4a (441 mg, 1.5 mmol), DIPEA (0.78 mL, 4.5 mmol), and Fmoc-OSu (455 mg, 1.35 mmol) were reacted together to give 4b as a beige solid (300 mg, 99% yield). 1H NMR (300 MHz, $CDCl_3$) δ 7.77 (t, $J = 7.6$ Hz, 3H), 7.66–7.54 (m, 3H), 7.44–7.30 (m, 9H), 6.97 (d, $J = 8.3$ Hz, 2H), 5.77 (d, $J = 6.3$ Hz, 1H), 5.34 (d, $J = 6.4$ Hz, 1H), 5.05 (s, 2H), 4.39 (d, $J = 6.6$ Hz, 1H), 4.26–4.16 (m, 1H). HRMS (ESI): m/z $[M - H]^-$ calcd for $C_{30}H_{24}NO_5$, 478.1660; found, 478.1667.

*N*_α-Fmoc-[4-(4-cyano)benzyloxy]-*D*-phenylglycine (**5b**). Following the general procedure, **5a** (223 mg, 0.7 mmol), DIPEA (0.37 mL, 2.1 mmol), and Fmoc-OSu (213 mg, 0.63 mmol) were reacted together to give **5b** as a beige solid (270 mg, 85% yield). ¹H NMR (300 MHz, CDCl₃) δ 7.74 (t, *J* = 7.8 Hz, 3H), 7.67 (d, *J* = 8.2 Hz, 2H), 7.60–7.55 (m, 1H), 7.53 (d, *J* = 8.2 Hz, 2H), 7.45–7.29 (m, 4H), 7.17 (s, 2H), 6.92 (dd, *J* = 13.5, 8.5 Hz, 2H), 5.75 (d, *J* = 6.6 Hz, 1H), 5.35 (d, *J* = 6.6 Hz, 1H), 5.11 (s, 2H), 4.39 (d, *J* = 6.2 Hz, 2H), 4.25–4.15 (m, 1H). HRMS (ESI): *m/z* [M – H][–] calcd for C₃₁H₂₃N₂O₅, 503.1612; found, 503.1605.

*N*_α-Fmoc-[4-(4-bromo)benzyloxy]-*D*-phenylglycine (**6b**). Following the general procedure, **6a** (261 mg, 0.7 mmol), DIPEA (0.37 mL, 2.1 mmol), and Fmoc-OSu (213 mg, 0.63 mmol) were reacted together to give **6b** as a beige solid (340 mg, 97% yield). ¹H NMR (300 MHz, CDCl₃) δ 7.74 (t, *J* = 8.1 Hz, 2H), 7.57 (d, *J* = 7.0 Hz, 1H), 7.54–7.46 (m, 2H), 7.43–7.27 (m, 5H), 7.17 (s, 1H), 6.92 (dd, *J* = 11.7, 7.6 Hz, 2H), 5.75 (d, *J* = 6.6 Hz, 1H), 5.35 (d, *J* = 6.8 Hz, 1H), 5.00 (s, 2H), 4.39 (d, *J* = 5.0 Hz, 2H), 4.26–4.15 (m, 1H). HRMS (ESI): *m/z* [M – H][–] calcd for C₃₀H₂₃BrNO₅, 556.0765; found, 556.0741.

*N*_α-Fmoc-[4-(4-fluoro)benzyloxy]-*D*-phenylglycine (**7b**). Following the general procedure, **7a** (218 mg, 0.7 mmol), DIPEA (0.37 mL, 2.1 mmol), and Fmoc-OSu (213 mg, 0.63 mmol) were reacted together to give **7b** as a beige solid (300 mg, 96% yield). ¹H NMR (300 MHz, CDCl₃) δ 7.74 (t, *J* = 8.1 Hz, 2H), 7.57 (d, *J* = 7.0 Hz, 1H), 7.54–7.46 (m, 2H), 7.43–7.27 (m, 5H), 7.17 (s, 1H), 6.92 (dd, *J* = 11.7, 7.6 Hz, 2H), 5.75 (d, *J* = 6.6 Hz, 1H), 5.35 (d, *J* = 6.8 Hz, 1H), 5.00 (s, 2H), 4.39 (d, *J* = 5.0 Hz, 2H), 4.26–4.15 (m, 1H). HRMS (ESI): *m/z* [M – H][–] calcd for C₃₀H₂₃FNO₅, 496.1566; found, 496.1571.

*N*_α-Fmoc-[4-(4-chloro)benzyloxy]-*D*-phenylglycine (**8b**). Following the general procedure, **8a** (656 mg, 2 mmol), DIPEA (1.05 mL, 6 mmol), and Fmoc-OSu (607 mg, 1.8 mmol) were reacted together to give **8b** as a beige solid (596 mg, 64% yield). ¹H NMR (300 MHz, CDCl₃) δ 7.74 (t, *J* = 8.2 Hz, 2H), 7.57 (d, *J* = 6.6 Hz, 1H), 7.44–7.28 (m, 9H), 7.17 (s, 2H), 6.98–6.87 (m, 2H), 5.75 (d, *J* = 6.4 Hz, 1H), 5.35 (d, *J* = 6.7 Hz, 1H), 5.01 (s, 2H), 4.39 (d, *J* = 5.7 Hz, 2H), 4.26–4.13 (m, 1H). HRMS (ESI): *m/z* [M – H][–] calcd for C₃₀H₂₃ClNO₅, 512.1270; found, 512.1248.

*N*_α-Fmoc-[4-(4-trifluoromethyl)benzyloxy]-*D*-phenylglycine (**9b**). Following the general procedure, **9a** (181 mg, 0.5 mmol), DIPEA (0.26 mL, 1.5 mmol), and Fmoc-OSu (160 mg, 0.48 mmol) were reacted together to give **9b** as a beige solid (243 mg, 93% yield). ¹H NMR (300 MHz, CDCl₃) δ 7.74 (t, *J* = 8.1 Hz, 2H), 7.64 (d, *J* = 8.2 Hz, 2H), 7.55 (t, *J* = 8.7 Hz, 3H), 7.45–7.27 (m, 5H), 7.17 (s, 2H), 6.93 (dd, *J* = 12.3, 8.6 Hz, 2H), 5.75 (d, *J* = 6.5 Hz, 1H), 5.36 (d, *J* = 6.6 Hz, 1H), 5.11 (s, 2H), 4.39 (d, *J* = 5.9 Hz, 2H), 4.28–4.16 (m, 1H). HRMS (ESI): *m/z* [M – H][–] calcd for C₃₁H₂₃F₃NO₅, 546.1534; found, 546.1503.

*N*_α-Fmoc-[4-(4-trifluoromethoxy)benzyloxy]-*D*-phenylglycine (**10b**). Following the general procedure, **10a** (110 mg, 0.29 mmol), DIPEA (0.15 mL, 0.87 mmol), and Fmoc-OSu (93 mg, 0.28 mmol) were reacted together to give **10b** as a brown solid (135 mg, 86% yield). ¹H NMR (300 MHz, CDCl₃) δ 7.75 (d, *J* = 7.2 Hz, 2H), 7.62 (d, *J* = 7.7 Hz, 1H), 7.57 (d, *J* = 7.5 Hz, 1H), 7.45 (d, *J* = 8.6 Hz, 2H), 7.41–7.28 (m, 6H), 7.24 (d, *J* = 8.5 Hz, 2H), 6.96 (d, *J* = 8.4 Hz, 2H), 5.75 (d, *J* = 6.6 Hz, 1H), 5.35 (d, *J* = 6.8 Hz, 1H), 5.04 (s, 2H), 4.44–4.36 (m, 2H), 4.25–4.17 (m, 1H). HRMS (ESI): *m/z* [M – H][–] calcd for C₃₁H₂₃F₃NO₆, 562.1483; found, 562.1456.

*N*_α-Fmoc-[4-(2-bromo)benzyloxy]-*D*-phenylglycine (**11b**). Following the general procedure, **11a** (559 mg, 1.5 mmol), DIPEA (0.78 mL, 4.5 mmol), and Fmoc-OSu (455 g, 1.35 mmol) were reacted together to give **11b** as a beige solid (450 mg, 60% yield). ¹H NMR (300 MHz, CDCl₃) δ 7.74 (t, *J* = 8.3 Hz, 2H), 7.59 (dd, *J* = 7.9, 1.1 Hz, 2H), 7.52 (d, *J* = 7.8 Hz, 2H), 7.43–7.28 (m, 6H), 7.20 (dd, *J* = 7.9, 1.3 Hz, 2H), 6.95 (dd, *J* = 14.2, 8.3 Hz, 2H), 5.73 (d, *J* = 6.6 Hz, 1H), 5.36 (d, *J* = 6.8 Hz, 1H), 5.13 (s, 2H), 4.41 (d, *J* = 6.8 Hz, 2H), 4.26–4.16 (m, 1H). HRMS (ESI): *m/z* [M – H][–] calcd for C₃₀H₂₃BrNO₅, 556.0765; found, 555.0744.

*N*_α-Fmoc-[4-(2-trifluoromethyl)benzyloxy]-*D*-phenylglycine (**12b**). Following the general procedure, **12a** (362 mg, 1 mmol), DIPEA (0.52

mL, 3 mmol) and Fmoc-OSu (320 mg, 0.95 mmol) were reacted together to give **12b** as a beige solid (500 mg, 96% yield). ¹H NMR (300 MHz, CDCl₃) δ 7.90 (s, 1H), 7.78–7.68 (m, 4H), 7.62–7.51 (m, 2H), 7.43 (d, *J* = 7.7 Hz, 1H), 7.40–7.29 (m, 3H), 7.22 (d, *J* = 8.5 Hz, 1H), 7.18 (d, *J* = 3.2 Hz, 2H), 6.93 (dd, *J* = 16.7, 8.3 Hz, 2H), 5.73 (d, *J* = 6.9 Hz, 1H), 5.36 (d, *J* = 6.8 Hz, 1H), 5.27 (s, 2H), 4.43–4.36 (m, 2H), 4.25–4.16 (m, 1H). HRMS (ESI): *m/z* [M – H][–] calcd for C₃₁H₂₃F₃NO₅, 546.1534; found, 546.1538.

*N*_α-Fmoc-[4-(2-chloro)benzyloxy]-*D*-phenylglycine (**13b**). Following the general procedure, **13a** (492 mg, 1.5 mmol), DIPEA (0.78 mL, 4.5 mmol), and Fmoc-OSu (455 mg, 1.3 mmol) were reacted together to give **13b** as a light brown solid (680 mg, 98% yield). ¹H NMR (300 MHz, CDCl₃) δ 7.75 (d, *J* = 7.3 Hz, 2H), 7.63–7.48 (m, 3H), 7.44–7.30 (m, 5H), 7.28 (d, *J* = 3.6 Hz, 2H), 7.22 (d, *J* = 8.9 Hz, 2H), 6.98 (d, *J* = 8.4 Hz, 2H), 5.79 (d, *J* = 6.6 Hz, 1H), 5.34 (d, *J* = 6.8 Hz, 1H), 5.16 (s, 2H), 4.46–4.33 (m, 2H), 4.25–4.16 (m, 1H). HRMS (ESI): *m/z* [M – H][–] calcd for C₃₀H₂₃ClNO₅, 512.1259; found, 512.1268.

*N*_α-Fmoc-[4-(3-chloro)benzyloxy]-*D*-phenylglycine (**14b**). Following the general procedure, **14a** (328 mg, 1 mmol), DIPEA (0.52 mL, 3 mmol), and Fmoc-OSu (304 mg, 0.9 mmol) were reacted together to give **14b** as a beige solid (450 mg, 97% yield). ¹H NMR (300 MHz, CDCl₃) δ 7.88 (s, 1H), 7.74 (t, *J* = 8.7 Hz, 2H), 7.57 (d, *J* = 7.1 Hz, 1H), 7.48–7.31 (m, 6H), 7.30 (d, *J* = 1.2 Hz, 2H), 7.17 (d, *J* = 3.2 Hz, 2H), 6.98–6.88 (m, 2H), 5.74 (d, *J* = 6.7 Hz, 1H), 5.35 (d, *J* = 6.8 Hz, 1H), 5.02 (s, 2H), 4.39 (d, *J* = 5.9 Hz, 2H), 4.27–4.15 (m, 1H). HRMS (ESI): *m/z* [M – H][–] calcd for C₃₀H₂₃ClNO₅, 512.1270; found, 512.1240.

*N*_α-Fmoc-[4-(2,6-dichloro)benzyloxy]-*D*-phenylglycine (**15b**). Following the general procedure, **15a** (363 mg, 1 mmol), DIPEA (0.52 mL, 3 mmol), and Fmoc-OSu (321 mg, 0.95 mmol) were reacted together to give **15b** as a beige solid (500 mg, 96% yield). ¹H NMR (300 MHz, CDCl₃) δ 7.80–7.68 (m, 2H), 7.58 (d, *J* = 7.1 Hz, 1H), 7.44–7.39 (m, 1H), 7.37 (dd, *J* = 8.2, 1.6 Hz, 2H), 7.35–7.27 (m, 4H), 7.24 (dd, *J* = 8.1, 1.8 Hz, 1H), 7.20–7.11 (m, 2H), 7.08–6.95 (m, 2H), 5.75 (d, *J* = 6.7 Hz, 1H), 5.38 (d, *J* = 6.6 Hz, 1H), 5.27 (s, 2H), 4.42 (d, *J* = 6.9 Hz, 2H), 4.27–4.18 (m, 1H). HRMS (ESI): *m/z* [M – H][–] calcd for C₃₀H₂₂Cl₂NO₅, 546.0881; found, 546.0868.

*N*_α-Fmoc-[4-(3,4-dichloro)benzyloxy]-*D*-phenylglycine (**16b**). Following the general procedure, **16a** (254 mg, 0.7 mmol), DIPEA (0.37 mL, 2.1 mmol), and Fmoc-OSu (224 mg, 0.67 mmol) were reacted together to give **16b** as a light brown solid (360 mg, 98% yield). ¹H NMR (300 MHz, CDCl₃) δ 7.74 (t, *J* = 7.8 Hz, 2H), 7.62–7.51 (m, 2H), 7.45 (d, *J* = 8.2 Hz, 1H), 7.43–7.27 (m, 5H), 7.23 (s, 1H), 7.17 (s, 2H), 6.91 (dd, *J* = 11.5, 8.6 Hz, 2H), 5.75 (d, *J* = 6.7 Hz, 1H), 5.35 (d, *J* = 6.7 Hz, 1H), 4.99 (s, 2H), 4.44–4.35 (m, 2H), 4.25–4.16 (m, 1H). HRMS (ESI): *m/z* [M – H][–] calcd for C₃₀H₂₂Cl₂NO₅, 546.0881; found, 546.0860.

*N*_α-Fmoc-[4-(3-methoxy)benzyloxy]-*D*-phenylglycine (**17b**). Following the general procedure, **17a** (486 mg, 1.5 mmol), DIPEA (0.78 mL, 4.5 mmol), and Fmoc-OSu (455 mg, 1.35 mmol) were reacted together to give **17b** as a light brown solid (650 mg, 95% yield). ¹H NMR (300 MHz, CDCl₃) δ 7.79–7.69 (m, 2H), 7.57 (d, *J* = 7.2 Hz, 1H), 7.45–7.26 (m, 6H), 7.18 (s, 2H), 7.04–6.91 (m, 4H), 6.87 (dd, *J* = 7.8, 2.2 Hz, 1H), 5.72 (d, *J* = 6.5 Hz, 1H), 5.35 (d, *J* = 6.8 Hz, 1H), 5.03 (s, 2H), 4.37 (d, *J* = 14.2 Hz, 2H), 4.25–4.15 (m, 1H), 3.81 (s, 3H). HRMS (ESI): *m/z* [M – H][–] calcd for C₃₁H₂₆NO₆, 508.1766; found, 508.1752.

*N*_α-Fmoc-[4-(3-methyl)benzyloxy]-*D*-phenylglycine (**18b**). Following the general procedure, **18a** (616 mg, 2 mmol), DIPEA (1.05 mL, 6 mmol), and Fmoc-OSu (607 mg, 1.8 mmol) were reacted together to give **18b** as a beige solid (860 mg, 97% yield). ¹H NMR (300 MHz, CDCl₃) δ 7.84 (s, 1H), 7.74 (t, *J* = 8.7 Hz, 2H), 7.57 (d, *J* = 7.1 Hz, 1H), 7.47–7.31 (m, 4H), 7.29 (d, *J* = 7.4 Hz, 2H), 7.24 (d, *J* = 3.4 Hz, 2H), 7.14 (d, *J* = 7.4 Hz, 2H), 7.02–6.90 (m, 2H), 5.73 (d, *J* = 6.8 Hz, 1H), 5.35 (d, *J* = 6.8 Hz, 1H), 5.01 (s, 2H), 4.46–4.33 (m, 2H), 4.25–4.16 (m, 1H), 2.37 (s, 3H). HRMS (ESI): *m/z* [M – H][–] calcd for C₃₁H₂₆NO₅, 492.1816; found, 492.1804.

*N*_α-Fmoc-[4-(4-tert-butyl)benzyloxy]-*D*-phenylglycine (**19b**). Following the general procedure, **19a** (670 mg, 2 mmol), DIPEA (1.05 mL, 6 mmol), and Fmoc-OSu (1.21 g, 1.9 mmol) were reacted

together to give **19b** as a beige solid (980 mg, 96% yield). ^1H NMR (300 MHz, CDCl_3) δ 7.79–7.70 (m, 2H), 7.58 (d, J = 7.0 Hz, 1H), 7.42 (d, J = 8.4 Hz, 2H), 7.39–7.27 (m, 6H), 7.23 (s, 1H), 7.17 (s, 2H), 7.00–6.89 (m, 2H), 5.77 (d, J = 6.7 Hz, 1H), 5.35 (d, J = 6.8 Hz, 1H), 5.01 (s, 2H), 4.41 (d, J = 6.8 Hz, 2H), 4.26–4.17 (m, 1H), 1.33 (s, 9H). HRMS (ESI): m/z $[\text{M} - \text{H}]^-$ calcd for $\text{C}_{34}\text{H}_{32}\text{NO}_5$, 534.2286; found, 534.2262.

N_α -Fmoc-[4-(naphth-2-yl)methoxy]-*D*-phenylglycine (**20b**). Following the general procedure with the addition of 10 mL of DMSO to improve the starting material solubility, **20a** (138 mg, 0.4 mmol), DIPEA (0.21 mL, 1.2 mmol), and Fmoc-OSu (130 mg, 0.39 mmol) were reacted together to give **20b** as a yellow solid (194 mg, 95% yield). ^1H NMR (300 MHz, CDCl_3) δ 7.89–7.82 (m, 4H), 7.75 (d, J = 7.6 Hz, 2H), 7.60–7.53 (m, 2H), 7.49 (dd, J = 8.1, 4.4 Hz, 3H), 7.43–7.28 (m, 6H), 7.01 (d, J = 8.1 Hz, 2H), 5.78 (d, J = 6.6 Hz, 1H), 5.34 (d, J = 6.8 Hz, 1H), 5.22 (s, 2H), 4.42–4.32 (m, 2H), 4.24–4.17 (m, 1H). HRMS (ESI): m/z $[\text{M} - \text{H}]^-$ calcd for $\text{C}_{34}\text{H}_{26}\text{NO}_5$, 528.1816; found, 528.1796.

N_α -Fmoc-4-(phenacyloxy)-*D*-phenylglycine (**21b**). Following the general procedure, **21a** (225 mg, 0.7 mmol), DIPEA (0.37 mL, 2.1 mmol), and Fmoc-OSu (213 mg, 0.63 mmol) were reacted together to give **21b** as a brown solid (220 mg, 69% yield). ^1H NMR (300 MHz, CDCl_3) δ 8.06–7.96 (m, 2H), 7.75 (d, J = 7.3 Hz, 2H), 7.67–7.48 (m, 5H), 7.42–7.32 (m, 4H), 6.93 (d, J = 8.5 Hz, 2H), 6.81 (d, J = 8.3 Hz, 2H), 5.74 (d, J = 6.6 Hz, 1H), 5.34 (s, 1H), 5.29 (d, J = 6.3 Hz, 2H), 4.43–4.37 (m, 2H), 4.24–4.17 (m, 1H). HRMS (ESI): m/z $[\text{M} - \text{H}]^-$ calcd for $\text{C}_{31}\text{H}_{24}\text{NO}_6$, 506.1609; found, 506.1587.

N_α -Fmoc-[4-(4-bromophenacyloxy)]-*D*-phenylglycine (**22b**). Following the general procedure, **22a** (361 mg, 0.9 mmol), DIPEA (0.47 mL, 3 mmol), and Fmoc-OSu (273 mg, 0.81 mmol) were reacted together to give **22b** as a yellow solid (390 mg, 82% yield). ^1H NMR (300 MHz, CDCl_3) δ 7.86 (dd, J = 8.6, 2.0 Hz, 2H), 7.75 (d, J = 7.5 Hz, 2H), 7.64 (dd, J = 8.4, 2.2 Hz, 2H), 7.57 (d, J = 6.2 Hz, 2H), 7.40–7.30 (m, 6H), 6.91 (d, J = 7.6 Hz, 2H), 5.75 (d, J = 4.9 Hz, 1H), 5.35 (d, J = 5.1 Hz, 1H), 5.20 (s, 2H), 4.40 (d, J = 6.5 Hz, 2H), 4.24–4.18 (m, 1H). HRMS (ESI): m/z $[\text{M} - \text{H}]^-$ calcd for $\text{C}_{31}\text{H}_{23}\text{BrNO}_6$, 584.0714; found, 584.0689.

N_α -Fmoc- N_ϵ -Boc-[4-(4-amino)benzyloxy]-*D*-phenylglycine (**108b**). Following the general procedure, **108a** (82 mg, 0.2 mmol), DIPEA (0.11 mL, 0.6 mmol), and Fmoc-OSu (64 mg, 0.19 mmol) were reacted together to give **108b** as a yellow solid (95 mg, 84% yield). ^1H NMR (300 MHz, CDCl_3) δ 7.75 (d, J = 7.5 Hz, 2H), 7.58 (d, J = 7.2 Hz, 2H), 7.43–7.28 (m, 11H), 6.95 (d, J = 8.2 Hz, 2H), 6.53 (s, 1H), 5.35 (d, J = 6.4 Hz, 1H), 5.00 (s, 2H), 4.40 (d, J = 6.6 Hz, 2H), 4.24–4.18 (m, 1H), 1.52 (s, 9H). HRMS (ESI): m/z $[\text{M} - \text{H}]^-$ calcd for $\text{C}_{35}\text{H}_{33}\text{N}_2\text{O}_7$, 593.2293; found, 593.2294.

General Procedure for the Synthesis of Peptide Hybrids. All peptide and peptide hybrid sequences were assembled by stepwise solid-phase synthesis on Rink amide resin using the standard Fmoc-strategy, as previously described.^{29–31,39} Solid phase synthesis was done manually in plastic syringes equipped with a frit; all steps were performed at room temperature under continuous shaking. The Rink amide resin (loading capacity 0.64 mmol/g) was preswollen in DCM for at least 30 min and then washed 3 \times with DMF. For Fmoc group deprotection, a piperidine solution (25% in DMF) was added 2 \times for 10 and 5 min. Following each deprotection or coupling step, the resin was washed 3 \times with DMF, 3 \times with DCM, and again 3 \times with DMF. HATU/DIPEA were used for coupling steps. In detail, the coupling solution contained the N_α -Fmoc-protected amino acid or N-terminal carboxylic acid capping group (3 equiv), HATU (3 equiv), and DIPEA (4 equiv) in DMF (~1.0 mL per 100 mg of resin). The solution was added to the resin, and the reaction was shaken for 45–90 min. Afterward, the resin was washed as described before. Fmoc deprotection and coupling steps were iteratively repeated until the desired sequence was obtained. For the synthesis of peptide hybrids sharing an identical amino acid sequence but differing in the N-terminal cap, the Fmoc-protected peptide sequence was synthesized on a large scale, split, and stored at 4 $^\circ\text{C}$ until use. For the sequences containing 4-(OH)-phenylglycine (**24–25**), a final treatment with piperidine solution (25% in DMF) for 30 min was carried out after

coupling of the N-terminal cap to cleave any formed esters at the unprotected hydroxyl group.

The resin loaded with the finished peptide or peptide hybrid was washed 3 \times with diethyl ether and dried under reduced pressure. The final product was cleaved off the resin with TFA/triisopropylsilane/water solution (95:1:4, 1–2 mL per 100 mg resin), and the mixture was shaken for at least 2 h. The cleavage solution was dispensed into cold diethyl ether (20 mL per 100 mg of resin), and the resulting precipitate was centrifuged (4000g, 10 min), washed with diethyl ether, and dried under reduced pressure. All crude peptides were purified by preparative HPLC on an ÄKTA Purifier, GE Healthcare (Germany), with an RP-18 pre and main column (Rephosphor, Dr. Maisch GmbH, Germany, C18-DE, 5 μm , 30 mm \times 16 mm and 120 mm \times 16 mm). The following conditions were used: eluent A, water (0.1% TFA); eluent B, methanol (0.1% TFA); flow rate, 8 mL/min; and gradient, 10% B (2.5 min), 100% B (23.5 min), 100% B (26 min), 10% B (26.1 min), and 10% B (30 min). Detection was performed at 214, 254, and 280 nm. After purification, methanol was evaporated, and the peptides were freeze-dried in water and stored at -20 $^\circ\text{C}$.

Expression and Purification of DENV and WNV Proteases. DENV (serotype 2) and WNV NS2B-NS3 protease constructs possessing a glycine-serine GGGSGGGG linker, which covalently connects the NS3 protease and NS2B cofactor domains, were used.^{55,56} Both viral proteases were expressed and purified following the protocol described by Steuer et al.^{57,58}

FRET Substrates Synthesis. Dengue and WNV protease FRET substrates, with the sequences 2-Abz-Nle-Lys-Arg-Arg-Ser-(3- NO_2)-Tyr-NH $_2$ for DENV (K_m 105 μM) and 2-Abz-Gly-Leu-Lys-Arg-Gly-Gly-(3- NO_3)-Tyr-NH $_2$ for WNV (K_m 212 μM), were synthesized by solid phase peptide synthesis using Fmoc-strategy, as described for the dengue FRET substrate.³⁹ Purity was assessed by LC-MS using method B.

DENV and WNV Protease Assays. DENV and WNV protease assays were performed as previously described.^{30,39} The continuous enzymatic assays were performed in black 96 well V-bottom plates (Greiner Bio-One, Germany) on a BMG Labtech Fluostar OPTIMA Microtiter fluorescence plate reader using excitation and emission wavelengths of 320 and 405 nm, respectively. The inhibitors (final concentration 50 μM , from 10 mM stock solutions in DMSO) were preincubated for 15 min with the DENV protease (100 nM) or WNV protease (150 nM) in the assay buffer (50 mM Tris-HCl pH 9, ethylene glycol (10% v/v), and 0.0016% Brij 58). Subsequently, the reaction was initiated by the addition of the FRET substrate (final concentration 50 μM) to obtain a final assay volume 100 μL per well. The enzymatic activity was determined as slope per second (relative fluorescence units per second) and monitored for 15 min. Percentage inhibition was calculated relative to a positive control (without the inhibitor). All experiments were performed in triplicate and averaged.

HPLC-Based DENV and WNV Protease Assays. After performing the fluorimetric assay (15 min), the enzymatic reaction was stopped by adding 10 μL of TFA (4%) to each well, and the samples were cooled to 4 $^\circ\text{C}$ for 30 min. The HPLC analysis was carried out on a Jasco HPLC system equipped with a RP-18 column Phenomenex Luna C18(2) (5 μm , 150 \times 3 mm) and a FP-2020 plus fluorescence detector (excitation, 320 nm; emission, 405 nm). The following conditions were used for DENV assay as previously described:^{30,39} flow rate, 1.0 mL/min; eluent A, water (0.1% TFA); eluent B, acetonitrile (0.1% TFA); and gradient, 10% B (0 min), 10% B (1 min), 95% B (9.5 min), 95% B (9.6 min), 10% B (12.6 min), and 10% B (15 min). Different conditions were used for the WNV assay: flow rate, 1.2 mL/min; eluent A, water (0.1% TFA); eluent B, acetonitrile (0.1% TFA); and gradient, 10% B (0 min), 20% B (1 min), 95% B (5 min), 95% B (6 min), 10% B (6.1 min), and 10% B (8 min). Percentage inhibition was calculated relative to a positive control (without the inhibitor). All experiments were performed in triplicate and averaged.

IC_{50} and K_i Determination. For determination of the half maximal inhibitory concentrations (IC_{50}), according to the compound percent inhibition at 50 μM , eight inhibitor concentrations covering the range 0–1, 0–2, 0–6, or 0–50 μM were chosen for analysis. Determinations were carried out in triplicate, and IC_{50} -values were determined for a

substrate concentration of 50 μM using Prism 5.0 (Graphpad Software, Inc.). For DENV, an enzyme concentration of 30 nM was used for IC_{50} determination, except for **83** and **86**, where an enzyme concentration of 15 nM was used. For WNV, IC_{50} -values were determined at an enzyme concentration of 75 nM, except for **83** where an enzyme concentration of 40 nM was used. For the calculation of the dissociation constant of the enzyme–inhibitor complex (K_i -value), IC_{50} -values at different substrate concentrations (50, 100, 150, and 200 μM) were plotted against their corresponding substrate concentrations (Cheng–Prusoff equation),^{46,59} and linear regression (considering the standard deviations) was performed using OriginPro 8.5 (OriginLab Corp.).

Cell Viability Assay. Huh-7 cells (10^4) per well were seeded into 96 well plates in 50 μL of DMEM supplemented with 10% FBS and incubated overnight at 37 °C. Following this, the cells were infected with WT DENV serotype 2 with an MOI of 1 or with WT WNV with an MOI of 0.1 in the presence of the respective concentration of the tested compound. Each concentration was assayed in triplicate. After incubation for 48 h at 37 °C, the medium was harvested; the triplicates were pooled and stored at –80 °C. Then, 50 μL of fresh DMEM was added to the cells, and cell viability was determined using Cell-Titer Glo Luminescent Viability Assay. A gradient of nontoxic concentrations was used for the determination of the virus yield reduction by the plaque assay using Vero E6 cells.

Virus Yield Reduction Assay. Vero E6 cells were seeded in 24 well plates with a density of 2.5×10^5 cells per well in DMEM supplemented with 10% FBS. After overnight incubation at 37 °C, the cells were infected with the harvested virus supernatant. The virus containing medium was diluted with DMEM ranging from 10^{-1} to 10^{-6} for DENV and from 10^{-2} to 10^{-7} for WNV before infection. After incubation of the cells with 100 μL of the virus dilution at 37 °C with agitation for 1 h, the medium was removed, and 1 mL of plaque medium was added. After further incubation for 7 days for DENV or 3 days for WNV at 37 °C, the cells were fixed with 5% (v/v) formaldehyde for 2 h, stained with crystal violet, and plaques were counted. EC_{50} values were calculated with OriginPro 8.5 using a nonlinear dose–response curve fit.

The correlation between EC_{50} values (μM) from the DENV-2 viral titer reduction assay and IC_{50} values (nM) at DENV-2 protease was performed using OriginPro 8.5 (OriginLab Corp.).

Parallel Artificial Membrane Permeability Assay (PAMPA). The permeability was evaluated for 12 compounds (**27**, **77**, **83**, **86**, **88**, **90**, **93**, **97**, **100**, **101**, **104**, and **105**), as described before,³³ using a precoated PAMPA plate system (BD Gentest, BD Bioscience, Germany). Phosphate buffered saline (PBS) (Sigma-Aldrich, Germany) was used for all experiments. Concentration determinations were carried out on a Jasco HPLC system with a UV-detector and an RP-18 column (ReproSil-Pur-ODS-3, Dr. Maisch GmbH, Germany, 5 μm , 50 mm \times 2 mm). The conditions for the method used were eluent A, water (0.1% TFA); eluent B, acetonitrile (0.1% TFA); and gradient, 1% B (0.2 min), 100% B (3.5 min), 100% B (4.5 min), 1% B (4.6 min), and 1% B (5 min). UV-detection was performed at 254 nm. Six-point calibration curves (10, 25, 50, 100, 150, and 200 μM) were generated for all analyzed compounds and references (amiloride, caffeine, and phenytoin) with correlation coefficients (R^2) being at least 0.99. The PAMPA system was warmed to room temperature for 1 h. In the donor plate, 300 μL of the 200 μM compound solutions in PBS was dispensed in triplicate, and in the acceptor plate, 200 μL of PBS buffer was added to all wells. The plates were combined, and the system was incubated at room temperature for 5 h. After incubation, 100 μL samples from each of the donor and acceptor wells are transferred into 96 well U-bottomed polypropylene plates (Greiner Bio-One, Germany) and quantitatively analyzed by UV absorbance on HPLC. The concentrations were determined from the previously generated calibration curves. Permeability (P_e) and mass retention (R) were calculated as described in the literature.^{51,52}

Metabolic Stability in Liver Microsomes. Metabolic stability for 3 compounds (**83**, **88**, and **104**) were performed as described before,³³ using pooled liver microsomes from male Sprague–Dawley rats (Sigma-Aldrich, Germany). In short, liver microsomal proteins (0.2

mg/mL) were supplemented with NADPH (10 mM) in DPBS (Dulbecco's phosphate buffered saline (Life Technologies, Germany)) and preincubated at 37 °C for 15 min. The analyzed compounds (100 μM) were added, and the samples were incubated at 37 °C for 30 min. Aliquots were removed at various time points (0, 2, 5, 10, 20, and 30 min). The reaction was terminated by the addition of an equal volume of acetonitrile, and the samples were cooled on ice for 15 min before centrifugation (4,500g at 4 °C for 15 min). The supernatants were used for further analysis. The loss of parent compound was monitored by HPLC on a Jasco HPLC system with a UV detector and RP-18 column (ReproSil-Pur-ODS, Dr. Maisch GmbH, Germany, 3 μm , 50 \times 2 mm) using the following method: eluent A, water (+0.1% TFA); eluent B, acetonitrile (+0.1% TFA); flow rate, 1 mL/min; and gradient, 1% B (0.2 min), 100% B (3.5 min), 100% B (4.5 min), 1% B (4.6 min), and 1% B (5 min). The metabolic stability was determined by dividing the peak areas of the unaltered parent compound in the metabolized sample by the peak areas of the parent compound in the reference sample. The activity of the microsomal preparations was verified by a positive control (testosterone).

Docking Studies. Autodock Vina 1.1.2 (AD Vina)⁴⁷ was used to perform the docking studies and investigate the binding mode of the most active compound (**83**). All calculations were performed on an Intel(R) Core(TM) i5-2450 M CPU at 2.50 GHz. The ligand was initially prepared using Chem3D Pro (PerkinElmer). For DENV, the crystal structure (3U11)⁴⁸ of the NS2B-NS3 protease of serotype 3 in complex with a tetrapeptidyl aldehyde was extracted from the dimer, and the sulfate ions and water molecules were removed. For the WNV, the crystal structure (2FP7)¹⁰ of the NS2B-NS3 protease in complex with the tetrapeptidyl aldehyde was used, and water molecules were removed. Docking preparation was performed with Autodock Tools.⁶⁰ Using default settings, polar hydrogen atoms were added, nonpolar hydrogen atoms were merged, and Kollman charges were assigned to the protein or Gasteiger charges to the ligand. AD Vina was used with docking parameters at default values. The grid spacing was 1.0, and the size of the docking grid was 25 Å for dengue and WNV. Visualization was performed with UCSF Chimera.⁶¹

■ ASSOCIATED CONTENT

📄 Supporting Information

The Supporting Information is available free of charge on the ACS Publications website at DOI: 10.1021/acs.jmedchem.5b01441.

Synthesis of derivatives **107a** and **107b**, thrombin and trypsin screening results, binding mode analysis by tryptophan quenching assays, kinetic studies, HRMS and HPLC data for all synthesized peptides, characterization of fluorescent compounds, NMR data for selected peptides, in addition to ¹H and ¹³C NMR spectra (PDF) SMILES data (CSV)

■ AUTHOR INFORMATION

Corresponding Author

*Phone: +49-6221-544875. Fax: +49-6221-546430. E-mail: c.klein@uni-heidelberg.de.

Notes

The authors declare no competing financial interest.

■ ACKNOWLEDGMENTS

We thank Heiko Rudy for measuring ESI high resolution spectra, Lena Weigel for performing LC-MS analytics, and Natascha Stefan for technical support. M.B. appreciates financial support from the German Academic Exchange Service. The project was sponsored by the Deutsche Forschungsgemeinschaft, KL-1356/3-1.

■ ABBREVIATIONS USED

Boc, *tert*-butoxycarbonyl; DENV, dengue virus; DIPEA, *N,N*-diisopropylethylamine; Fmoc, 9-fluorenylmethoxycarbonyl; Fmoc-OSu, *N*-(9-fluorenylmethoxycarbonyloxy)succinimide; FRET, Förster (fluorescence) resonance energy transfer; HATU, 1-[bis(dimethylamino)methylene]-1*H*-1,2,3-triazolo-[4,5-*b*]pyridinium 3-oxid hexafluorophosphate; HCV, hepatitis C virus; PAMPA, parallel artificial permeability assay; Phg, phenylglycine; RP-HPLC, reverse-phase high performance liquid chromatography; THR, thrombin; t_R , retention time; WNV, West Nile virus

■ REFERENCES

- (1) World Health Organization. Dengue and Severe Dengue, Fact Sheet No. 117. <http://www.who.int/mediacentre/factsheets/fs117/en/> (accessed on Jun 9, 2015).
- (2) Bhatt, S.; Gething, P. W.; Brady, O. J.; Messina, J. P.; Farlow, A. W.; Moyes, C. L.; Drake, J. M.; Brownstein, J. S.; Hoen, A. G.; Sankoh, O.; Myers, M. F.; George, D. B.; Jaenisch, T.; Wint, G. R. W.; Simmons, C. P.; Scott, T. W.; Farrar, J. J.; Hay, S. I. The Global Distribution and Burden of Dengue. *Nature* **2013**, *496*, 504–507.
- (3) Mitka, M. Dengue More Prevalent Than Previously Thought. *JAMA* **2013**, *309*, 1882–1882.
- (4) Chancey, C.; Grinev, A.; Volkova, E.; Rios, M. The Global Ecology and Epidemiology of West Nile Virus. *BioMed Res. Int.* **2015**, *2015*, 1.
- (5) Nitsche, C.; Holloway, S.; Schirmeister, T.; Klein, C. D. Biochemistry and Medicinal Chemistry of the Dengue Virus Protease. *Chem. Rev.* **2014**, *114*, 11348–11381.
- (6) Kilpatrick, A. M. Globalization, Land Use, and the Invasion of West Nile Virus. *Science* **2011**, *334*, 323–327.
- (7) Vasilakis, N.; Ooi, M.; Rabaa, M.; Mayer, S.; Widén, S.; Perera, D.; Hickey, A.; Travassos Da Rosa, A.; Bossart, K.; Tesh, R.; Holmes, E.; Cardoso, J. *The Daemon in the Forest - Emergence of a New Dengue Serotype in Southeast Asia, III*; International Conference on Dengue and Dengue Haemorrhagic Fever, Bangkok, Thailand, Oct 21–23, 2013.
- (8) Falgout, B.; Pethel, M.; Zhang, Y. M.; Lai, C. J. Both Nonstructural Proteins NS2B and NS3 are Required for the Proteolytic Processing of Dengue Virus Nonstructural Proteins. *J. Virol.* **1991**, *65*, 2467–2475.
- (9) Shiryayev, S. A.; Strongin, A. Y. Structural and Functional Parameters of the Flaviviral Protease: A Promising Antiviral Drug Target. *Future Virol.* **2010**, *5*, 593–606.
- (10) Erbel, P.; Schiering, N.; D'Arcy, A.; Renatus, M.; Kroemer, M.; Lim, S. P.; Yin, Z.; Keller, T. H.; Vasudevan, S. G.; Hommel, U. Structural Basis for the Activation of Flaviviral NS3 Proteases from Dengue and West Nile Virus. *Nat. Struct. Mol. Biol.* **2006**, *13*, 372–373.
- (11) Skorenski, M.; Sienczyk, M. Viral Proteases as Targets for Drug Design. *Curr. Pharm. Des.* **2013**, *19*, 1126–1153.
- (12) Au, J. S.; Pockros, P. J. Novel Therapeutic Approaches for Hepatitis C. *Clin. Pharmacol. Ther.* **2014**, *95*, 78–88.
- (13) De Clercq, E. Anti-HIV Drugs: 25 Compounds Approved within 25 Years After the Discovery of HIV. *Int. J. Antimicrob. Agents* **2009**, *33*, 307–320.
- (14) Cregar-Hernandez, L.; Jiao, G.-S.; Johnson, A. T.; Lehrer, A. T.; Wong, T. A. S.; Margosiak, S. A. Small Molecule Pan-Dengue and West Nile Virus NS3 Protease Inhibitors. *Antiviral Chem. Chemother.* **2011**, *21*, 209–218.
- (15) Shi, P. Y.; Yin, Z.; Nilar, S.; Keller, T. Dengue Drug Discovery. In *Third World Diseases*; Elliott, R., Ed.; Springer: Berlin, Germany, 2011; Vol. 7, pp 243–275.
- (16) Mueller, N. H.; Yon, C.; Ganesh, V. K.; Padmanabhan, R. Characterization of the West Nile Virus Protease Substrate Specificity and Inhibitors. *Int. J. Biochem. Cell Biol.* **2007**, *39*, 606–614.
- (17) Shiryayev, S. A.; Ratnikov, Boris, I.; Chekanov, Alexei, V.; Sikora, S.; Rozanov, Dmitri, V.; Godzik, A.; Wang, J.; Smith, Jeffrey, W.; Huang, Z.; Lindberg, I.; Samuel, Melanie A.; Diamond, Michael S.; Strongin, Alex, Y. Cleavage Targets and the D-Arginine-based Inhibitors of the West Nile Virus NS3 Processing Proteinase. *Biochem. J.* **2006**, *393*, 503–511.
- (18) Wu, H.; Bock, S.; Snitko, M.; Berger, T.; Weidner, T.; Holloway, S.; Kanitz, M.; Diederich, W. E.; Steuber, H.; Walter, C.; Hofmann, D.; Weißbrich, B.; Spannaus, R.; Acosta, E. G.; Bartenschlager, R.; Engels, B.; Schirmeister, T.; Bodem, J.; Novel Dengue. Virus NS2B/NS3 Protease Inhibitors. *Antimicrob. Agents Chemother.* **2014**, *59*, 1100–1109.
- (19) Liu, H.; Wu, R.; Sun, Y.; Ye, Y.; Chen, J.; Luo, X.; Shen, X.; Liu, H. Identification of Novel Thiadiazoloacrylamide Analogues as Inhibitors of Dengue-2 Virus NS2B/NS3 Protease. *Bioorg. Med. Chem.* **2014**, *22*, 6344–6352.
- (20) Schüller, A.; Yin, Z.; Brian Chia, C. S.; Doan, D. N. P.; Kim, H. K.; Shang, L.; Loh, T. P.; Hill, J.; Vasudevan, S. G. Tripeptide Inhibitors of Dengue and West Nile Virus NS2B–NS3 Protease. *Antiviral Res.* **2011**, *92*, 96–101.
- (21) Hammamy, M. Z.; Haase, C.; Hammami, M.; Hilgenfeld, R.; Steinmetzer, T. Development and Characterization of New Peptidomimetic Inhibitors of the West Nile Virus NS2B–NS3 Protease. *ChemMedChem* **2013**, *8*, 231–241.
- (22) Lim, S. P.; Shi, P. Y. West Nile Virus Drug Discovery. *Viruses* **2013**, *5*, 2977–3006.
- (23) Lim, S. P.; Wang, Q. Y.; Noble, C. G.; Chen, Y. L.; Dong, H.; Zou, B.; Yokokawa, F.; Nilar, S.; Smith, P.; Beer, D.; Lescar, J.; Shi, P. Y. Ten Years of Dengue Drug Discovery: Progress and Prospects. *Antiviral Res.* **2013**, *100*, 500–519.
- (24) Yin, Z.; Patel, S. J.; Wang, W. L.; Chan, W. L.; Ranga Rao, K. R.; Wang, G.; Ngew, X.; Patel, V.; Beer, D.; Knox, J. E.; Ma, N. L.; Ehrhardt, C.; Lim, S. P.; Vasudevan, S. G.; Keller, T. H. Peptide Inhibitors of Dengue Virus NS3 Protease. Part 2: SAR Study of Tetrapeptide Aldehyde Inhibitors. *Bioorg. Med. Chem. Lett.* **2006**, *16*, 40–43.
- (25) Yin, Z.; Patel, S. J.; Wang, W. L.; Wang, G.; Chan, W. L.; Rao, K. R.; Alam, J.; Jeyaraj, D. A.; Ngew, X.; Patel, V.; Beer, D.; Lim, S. P.; Vasudevan, S. G.; Keller, T. H. Peptide Inhibitors of Dengue Virus NS3 Protease. Part 1: Warhead. *Bioorg. Med. Chem. Lett.* **2006**, *16*, 36–39.
- (26) Knox, J. E.; Ma, N. L.; Yin, Z.; Patel, S. J.; Wang, W.-L.; Chan, W.-L.; Ranga Rao, K. R.; Wang, G.; Ngew, X.; Patel, V.; Beer, D.; Lim, S. P.; Vasudevan, S. G.; Keller, T. H. Peptide Inhibitors of West Nile NS3 Protease: SAR Study of Tetrapeptide Aldehyde Inhibitors. *J. Med. Chem.* **2006**, *49*, 6585–6590.
- (27) Yusof, R.; Clum, S.; Wetzel, M.; Murthy, H. M. K.; Padmanabhan, R. Purified NS2B/NS3 Serine Protease of Dengue Virus Type 2 Exhibits Cofactor NS2B Dependence for Cleavage of Substrates with Dibasic Amino Acids in Vitro. *J. Biol. Chem.* **2000**, *275*, 9963–9969.
- (28) Li, J.; Lim, S. P.; Beer, D.; Patel, V.; Wen, D.; Tumanut, C.; Tully, D. C.; Williams, J. A.; Jiricek, J.; Priestle, J. P.; Harris, J. L.; Vasudevan, S. G. Functional Profiling of Recombinant NS3 Proteases from All Four Serotypes of Dengue Virus Using Tetrapeptide and Octapeptide Substrate Libraries. *J. Biol. Chem.* **2005**, *280*, 28766–28774.
- (29) Nitsche, C.; Behnam, M. A. M.; Steuer, C.; Klein, C. D. Retro Peptide-Hybrids as Selective Inhibitors of the Dengue Virus NS2B–NS3 Protease. *Antiviral Res.* **2012**, *94*, 72–79.
- (30) Nitsche, C.; Schreier, V. N.; Behnam, M. A. M.; Kumar, A.; Bartenschlager, R.; Klein, C. D. Thiazolidinone–Peptide Hybrids as Dengue Virus Protease Inhibitors with Antiviral Activity in Cell Culture. *J. Med. Chem.* **2013**, *56*, 8389–8403.
- (31) Behnam, M. A. M.; Nitsche, C.; Vecchi, S. M.; Klein, C. D. C-Terminal Residue Optimization and Fragment Merging: Discovery of a Potent Peptide-Hybrid Inhibitor of Dengue Protease. *ACS Med. Chem. Lett.* **2014**, *5*, 1037–1042.

- (32) Bastos Lima, A.; Behnam, M. A. M.; El Sherif, Y.; Nitsche, C.; Vechi, S. M.; Klein, C. D. Dual Inhibitors of the Dengue and West Nile Virus NS2B–NS3 Proteases: Synthesis, Biological Evaluation and Docking Studies of Novel Peptide-Hybrids. *Bioorg. Med. Chem.* **2015**, *23*, 5748–5755.
- (33) Weigel, L. F.; Nitsche, C.; Graf, D.; Bartenschlager, R.; Klein, C. D. Phenylalanine and Phenylglycine Analogs as Arginine Mimetics in Dengue Protease Inhibitors. *J. Med. Chem.* **2015**, *58*, 7719–7733.
- (34) Wünsch, E.; Fries, G.; Zwick, A. Peptide Synthesis. V. Preparation and Use of O-Benzyl-L-Tyrosine in the Synthesis of Peptides. *Chem. Ber.* **1958**, *91*, 542–547.
- (35) Dawei, M.; Hongqi, T. Stereoselective Synthesis of (S)-(+)- α M4CPG, a Selective Antagonist of Metabotropic Glutamate Receptors. *Tetrahedron: Asymmetry* **1996**, *7*, 1567–1570.
- (36) Caplar, V.; Raza, Z.; Katalenic, D.; Zinic, M. Syntheses of Amino Alcohols and Chiral C2-Symmetric Bisoxazolines Derived from O-Alkylated R-4-Hydroxyphenylglycine and S-Tyrosine. *Croat. Chem. Acta* **2003**, *76*, 23–36.
- (37) Rzeszutarska, B.; Misiukiewicz, E.; Wiejak, S. A Process for Preparing *N*^ε-tert-Butoxycarbonyl-L-lysine. PL 194414, May 31, 2007.
- (38) Dener, J. M.; Fantauzzi, P. P.; Kshirsagar, T. A.; Kelly, D. E.; Wolfe, A. B. Large-Scale Syntheses of Fmoc-Protected Non-Proteogenic Amino Acids: Useful Building Blocks for Combinatorial Libraries. *Org. Process Res. Dev.* **2001**, *5*, 445–449.
- (39) Nitsche, C.; Klein, C. Fluorimetric and HPLC-Based Dengue Virus Protease Assays Using a FRET Substrate. In *Antiviral Methods and Protocols*; Gong, E. Y., Ed.; Humana Press: New York, 2013; Vol. 1030, pp 221–236.
- (40) Chorev, M.; Goodman, M. Recent Developments in Retro Peptides and Proteins — an Ongoing Topochemical Exploration. *Trends Biotechnol.* **1995**, *13*, 438–445.
- (41) Erlanson, D. A. Fragment-based Lead Discovery: A Chemical Update. *Curr. Opin. Biotechnol.* **2006**, *17*, 643–652.
- (42) Erlanson, D. A.; McDowell, R. S.; O'Brien, T. Fragment-based Drug Discovery. *J. Med. Chem.* **2004**, *47*, 3463–3482.
- (43) Hajduk, P. J.; Greer, J. A Decade of Fragment-based Drug Design: Strategic Advances and Lessons Learned. *Nat. Rev. Drug Discovery* **2007**, *6*, 211–219.
- (44) Joseph-McCarthy, D.; Campbell, A. J.; Kern, G.; Moustakas, D. Fragment-Based Lead Discovery and Design. *J. Chem. Inf. Model.* **2014**, *54*, 693–704.
- (45) Bodenreider, C.; Beer, D.; Keller, T. H.; Sonntag, S.; Wen, D.; Yap, L.; Yau, Y. H.; Shochat, S. G.; Huang, D.; Zhou, T.; Cafilisch, A.; Su, X.-C.; Ozawa, K.; Otting, G.; Vasudevan, S. G.; Lescar, J.; Lim, S. P. A Fluorescence Quenching Assay to Discriminate between Specific and Nonspecific Inhibitors of Dengue Virus Protease. *Anal. Biochem.* **2009**, *395*, 195–204.
- (46) Yung-Chi, C.; Prusoff, W. H. Relationship between the Inhibition Constant (KI) and the Concentration of Inhibitor Which Causes 50 per Cent Inhibition (I50) of an Enzymatic Reaction. *Biochem. Pharmacol.* **1973**, *22*, 3099–3108.
- (47) Trott, O.; Olson, A. J. AutoDock Vina: Improving the speed and accuracy of docking with a new scoring function, efficient optimization, and multithreading. *J. Comput. Chem.* **2010**, *31*, 455–461.
- (48) Noble, C. G.; Seh, C. C.; Chao, A. T.; Shi, P. Y. Ligand-Bound Structures of the Dengue Virus Protease Reveal the Active Conformation. *J. Virol.* **2012**, *86*, 438–446.
- (49) Giaginis, C.; Tsantili-Kakoulidou, A. Current State of the Art in HPLC Methodology for Lipophilicity Assessment of Basic Drugs. A Review. *J. Liq. Chromatogr. Relat. Technol.* **2007**, *31*, 79–96.
- (50) Dalvie, D. K.; Kalgutkar, A. S.; Khojasteh-Bakht, S. C.; Obach, R. S.; O'Donnell, J. P. Biotransformation Reactions of Five-Membered Aromatic Heterocyclic Rings. *Chem. Res. Toxicol.* **2002**, *15*, 269–299.
- (51) Kansy, M.; Senner, F.; Gubernator, K. Physicochemical High Throughput Screening: Parallel Artificial Membrane Permeation Assay in the Description of Passive Absorption Processes. *J. Med. Chem.* **1998**, *41*, 1007–1010.
- (52) Chen, X.; Murawski, A.; Patel, K.; Crespi, C.; Balimane, P. A Novel Design of Artificial Membrane for Improving the PAMPA Model. *Pharm. Res.* **2008**, *25*, 1511–1520.
- (53) Craik, D. J.; Fairlie, D. P.; Liras, S.; Price, D. The Future of Peptide-based Drugs. *Chem. Biol. Drug Des.* **2013**, *81*, 136–147.
- (54) Yan, Z.; Caldwell, G. W. Metabolic assessment in liver microsomes by co-activating cytochrome P450s and UDP-glycosyltransferases. *Eur. J. Drug Metab. Pharmacokinet.* **2003**, *28*, 223–232.
- (55) Leung, D.; Schroder, K.; White, H.; Fang, N. X.; Stoermer, M. J.; Abbenante, G.; Martin, J. L.; Young, P. R.; Fairlie, D. P. Activity of Recombinant Dengue 2 Virus NS3 Protease in the Presence of a Truncated NS2B Co-factor, Small Peptide Substrates, and Inhibitors. *J. Biol. Chem.* **2001**, *276*, 45762–45771.
- (56) Nall, T. A.; Chappell, K. J.; Stoermer, M. J.; Fang, N.-X.; Tyndall, J. D. A.; Young, P. R.; Fairlie, D. P. Enzymatic Characterization and Homology Model of a Catalytically Active Recombinant West Nile Virus NS3 Protease. *J. Biol. Chem.* **2004**, *279*, 48535–48542.
- (57) Steuer, C.; Heinonen, K. H.; Kattner, L.; Klein, C. D. Optimization of Assay Conditions for Dengue Virus Protease: Effect of Various Polyols and Nonionic Detergents. *J. Biomol. Screening* **2009**, *14*, 1102–1108.
- (58) Steuer, C.; Gege, C.; Fischl, W.; Heinonen, K. H.; Bartenschlager, R.; Klein, C. D. Synthesis and Biological Evaluation of α -Ketoamides as Inhibitors of the Dengue Virus Protease with Antiviral Activity in Cell-Culture. *Bioorg. Med. Chem.* **2011**, *19*, 4067–4074.
- (59) Newton, P.; Harrison, P.; Clulow, S. A Novel Method for Determination of the Affinity of Protein: Protein Interactions in Homogeneous Assays. *J. Biomol. Screening* **2008**, *13*, 674–682.
- (60) Morris, G. M.; Huey, R.; Lindstrom, W.; Sanner, M. F.; Belew, R. K.; Goodsell, D. S.; Olson, A. J. AutoDock4 and AutoDockTools4: Automated docking with selective receptor flexibility. *J. Comput. Chem.* **2009**, *30*, 2785–2791.
- (61) Pettersen, E. F.; Goddard, T. D.; Huang, C. C.; Couch, G. S.; Greenblatt, D. M.; Meng, E. C.; Ferrin, T. E. UCSF Chimera—A visualization system for exploratory research and analysis. *J. Comput. Chem.* **2004**, *25*, 1605–1612.